Carbonates in the Critical Zone

M. D. Covington[1,2], J. B. Martin[3], L. E. Toran[4], J. L. Macalady[5], N. Sekhon [6,7], P. L. Sullivan[8], Á. A. García, Jr.[9], J. B. Heffernan[10], and W. D. Graham[11]

[1]Department of Geosciences, University of Arkansas, Fayetteville, AR, USA. [2]ZRC SAZU, Karst Research Institute, Slovenia. [3]Department of Geological Sciences, University of Florida, Gainesville, FL, USA. [4]Department of Earth and Environmental Science, Temple University, Philadelphia, PA, USA [5]Department of Geosciences, Pennsylvania State University, State College, PA, USA [6]Department of Earth, Environmental and Planetary Science, Brown University, Providence 02908, Rhode Island, United States [7] Institute at Brown for Environment and Society, Brown University, Providence 02908, Rhode Island, United States [7]College of Earth, Ocean, and Atmospheric Science, Oregon State University, OR, USA [9]Department of Geology and Environmental Science, James Madison University, Harrisonburg, VA, USA [10]Nicholas School of the Environment, Duke University, Durham, NC [11]University of Florida Water Institute, Gainesville, FL, USA

Corresponding author: Matthew D. Covington (mcoving@uark.edu)

Key Points:

- A holistic understanding of Earth's critical zone requires integrative studies spanning the spectrum of carbonate and silicate landscapes.
- Porosity developed by congruent dissolution of carbonates decouples hillslopes from stream channels, altering topographic equilibrium.
- Shifts in carbonate critical zone structure from changing ecology, land use, and climate may be rapid because of fast dissolution kinetics.

Abstract

Earth's Critical Zone (CZ), the near-surface layer where rock is weathered and landscapes co-evolve with life, is profoundly influenced by the type of underlying bedrock. Previous studies employing the CZ framework have focused almost exclusively on landscapes dominated by silicate rocks. However, carbonate rocks crop out on approximately 15% of Earth's ice-free continental surface and provide important water resources and ecosystem services to ~1.2 billion people. Unlike silicates, carbonate minerals weather congruently and have high solubilities and rapid dissolution kinetics, enabling the development of large, interconnected pore spaces and preferential flow paths that restructure the CZ. Here we review the state of knowledge of the carbonate CZ, exploring parameters that produce contrasts in the CZ in different carbonate settings and identifying important open questions about carbonate CZ processes. We introduce the concept of a carbonate-silicate CZ spectrum and examine whether current conceptual models of the CZ, such as the conveyor model, can be applied to carbonate landscapes.We argue that, to advance beyond site-specific understanding and develop a more general conceptual framework for the role of carbonates in the CZ, we need integrative studies spanning both the carbonate-silicate spectrum and a range of carbonate settings.

Plain Language Summary

Carbonate landscapes, which cover ~15% of Earth's land surface and provide critical water resources and other services to ~1.2 billion people, require focused studies to understand how life and rocks interact. Most integrated studies of this "critical zone" focus on landscapes underlain by silicate minerals instead of considering the full spectrum of the minerals that make up bedrock. This review of the state of knowledge of the carbonate critical zone reveals that weathering extends to greater depths in carbonate landscapes compared with silicate landscapes, leading to the development of interconnected subsurface flow systems that transport both water and sediments. As a result, the flow of water and the movement of materials left behind by weathering rock may be disconnected from streams, unlike in silicate landscapes. Furthermore, changes in ecology, land use, and climate response may be rapid because carbonate dissolve faster than silicate rocks. Integrative studies of silicate, carbonate, and mixed silicate-carbonate landscapes will be required to further a holistic understanding of Earth's critical zone.

1 Introduction

The objectives of this paper are to review the state of knowledge of critical zone (CZ) processes in carbonate terrains, to advance a framework that serves to bridge the spectrum between carbonate and silicate CZ endmembers (Martin et al., 2021), and to identify key knowledge gaps in our understanding of the carbonate CZ. Earth's CZ is the region where landscapes co-evolve with life and is loosely defined as the zone from the base of continental crust weathering to the top of vegetation canopy (National Research Council, 2001). The CZ develops through interactions among geological, hydrological, chemical, biological, and climate processes. Understanding the scope of, and linkages between, these interactions requires interdisciplinary collaborations, to unravel how the CZ functions and responds to environmental perturbations, including human impacts on climate, land use, and global elemental cycling. As the concept of CZ science emerged, the U.S. scientific community engaged in focused research on Earth's CZ through the development of place-based Critical Zone Observatories (CZOs) (Brantley et al., 2017b), leading to the more recent development of theme-based Critical Zone

Networks (CZNs). The CZO/CZN sites span a variety of geological and climate settings across the U.S. However, the CZ framework is limited by a CZO/CZN focus on landscapes underlain by silicate rocks (Martin et al., 2021). Globally, scientists are beginning to establish CZ observatories on carbonate rocks (Gaillardet et al., 2018; Jourde et al., 2018; Quine et al., 2017), but carbonates remain underrepresented among the studies employing the CZ framework. Although prior and ongoing studies provide useful information about localized carbonate terrains, more synthesis and a better predictive understanding of the carbonate CZ will require integrative studies of multiple carbonate settings with varied characteristics. Such a synthesis could also improve fundamental understanding of the silicate dominated CZ, as weathering of carbonates is also important within (pre-)dominantly silicate settings (e.g. Brantley et al., 2013), and landscapes fall on a continuum between the carbonate and silicate endmembers.

A focus on terrains where the CZ is dominated by carbonate minerals is justified by their common occurrence, their influence on society and its resource base, and their role in the human experience and human culture. Approximately 15% of Earth's ice-free continental surface contains carbonate rock (Figure 1), and approximately 1.2 billion people, 16% of the Earth's population, reside on carbonate rock (Goldscheider et al., 2020). Landscapes developed by the dissolution of carbonate terrains, also known as karst, often appear as a central theme in cultural development among long-term communities around the world. Karst landforms and features have influenced Indigenous creation stories, place-naming (toponymy), culturally based geological interpretation, and local language adaptation in the Greater Antilles part of the Caribbean (Alvarez Nazario 1972; Dominguez-Cristobal 1989, 1992, 2007; Garcia et al., 2020; Pané 1999), as well as a form of wealth building in central Europe that goes back to the 17th century (Zorn et al., 2009). In addition, the conservation of karst features has become a global priority because they commonly link geological, ecological, cultural, archeological, and touristic resources (Williams, 2008a).

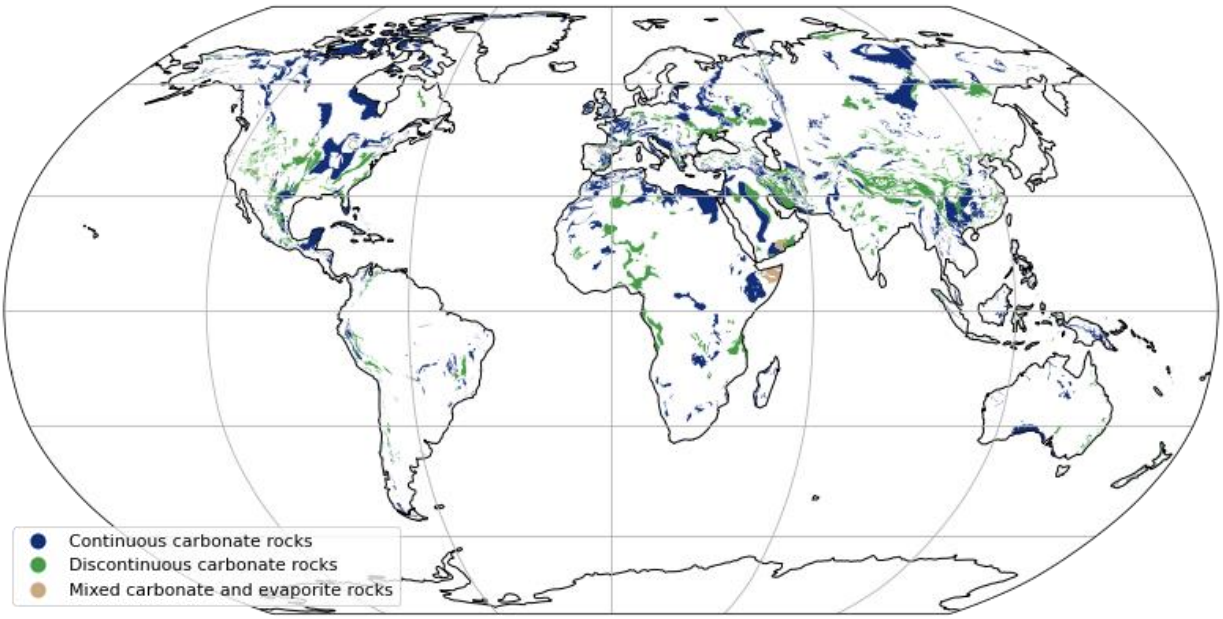

Figure 1. Carbonate exposures across the surface of earth using data from the World Karst Aquifer Map (data from Goldscheider et al., 2020). Areas with more than 65% carbonate rocks are mapped as continuous, whereas areas with between 15% and 65% carbonates are mapped

as discontinuous. Areas with greater than 15% of both carbonates and evaporites are mapped as mixed.

Carbonate terrains provide a wide range of societal and ecological services and present a variety of unique hazards. Given the favorable conditions for groundwater extraction from carbonates, and the ubiquity of springs within carbonate terrains, aquifers that develop in carbonate rocks are a crucial component of the global water supply (Ford and Williams, 2007; Worthington et al., 2016). Hazards unique to carbonate terrains, such as sinkholes and groundwater flooding, cause significant economic losses in densely populated areas (De Waele et al., 2011). Carbonate aquifers are particularly susceptible to contamination due to rapid travel times and limited natural remediation within large pores and conduits (White et al., 2016). Carbonate rocks are the largest global reservoir of carbon and have a potentially important, yet uncertain, role in the global carbon cycle over timescales relevant for rapid climate change (Baldini et al., 2018; Gaillardet et al., 2019; Martin, 2017). The raw materials for cement manufacturing are produced from carbonate rocks by calcination converting $CaCO_3$ to CaO plus CO_2, thereby producing 13% of the world's industrial CO_2 emissions (Fischedick et al., 2014). Carbonate minerals provide important pH buffering capacity within aquatic systems. Subterranean habitats within carbonate terrains host a wide variety of endemic species, many of which are threatened or endangered (Culver and Pipan, 2013). The carbonate CZ provides unique opportunities because of the ability for humans to access it at depth within caves. Interpretation of speleothem records within caves, which are an important source of paleoclimate information, requires substantial understanding of carbonate CZ processes, as signals recorded in speleothems are first filtered through the upper portion of the CZ (Fairchild et al., 2006; Fohlmeister et al., 2020). Consequently, studies of cave drip water have provided substantial insight into carbonate CZ dynamics (e.g., Tobin et al., 2021; Treble et al., 2022). Because of rapid mineral dissolution processes within, and subsurface fluxes through, the carbonate CZ, carbonate CZ systems may act as a bellwether for CZ responses to climatic and human perturbations (Sullivan et al., 2017). Furthermore, carbonate minerals often make up an important component of other sedimentary rocks (Hartmann and Moosdorf, 2012), and their distinct weathering characteristics can control weathering of non-carbonate minerals. The many impacts of carbonate minerals underscore the need for focused studies of carbonates in Earth's CZ.

2. Exploring the carbonate endmember

We begin with a review of current understanding of carbonate CZ processes. Within carbonate terrains, geological, hydrological, biological, geochemical, and climate variables produce a broad array of carbonate CZ characteristics. Here, we explore the range of parameters that create important differences within the carbonate CZ.

2.1 The importance of porosity distributions

Where the CZ occurs in nearly pure carbonate terrains, it is often transformed through congruent dissolution into karst, a landscape formed by dissolution of rock that develops underground drainage networks (Ford and Williams, 2007). Most karst landscapes form in carbonate bedrock, because of its common occurrence, although they also develop in evaporites (Klimchouk et al., 1996; Frumkin, 2013) and occasionally, in less soluble rocks (e.g., Wray and

Sauro, 2017). Dissolution integrates subsurface flow networks as water penetrates along heterogeneities in the rock until solutionally enlarged flow paths link input to outpoint points (Dreybrodt, 1990; Ford et al., 2000; Palmer, 1991). Such integrated flow paths, or karst conduits, are characterized by elevated permeability and exhibit rapid and turbulent flow that transports large quantities of solutes and gases between the surface and subsurface. High flow rates also allow the conduits to transport sediment through the subsurface (Cooper and Covington, 2020; Farrant and Smart, 2011; Herman et al., 2012). Once the capacity of the subsurface conduit network is sufficient to carry available surface runoff and sediment, closed basins develop on the land surface that route water and sediment into the subsurface. Conduit systems exit at springs, which frequently develop near the local hydrological base level. Together, these processes lead to the dolines, caves, and springs that characterize karst landscapes.

Karst aquifers are commonly conceptualized as a triple-porosity system, in which porosity is divided into a matrix component, a fracture component, and a conduit component (Quinlan et al., 1996; White, 2002; Worthington, 1999). The matrix component represents the primary porosity of the bedrock. The fracture component represents secondary porosity as a result of fractures and bedding partings. The conduit component represents dissolutionally enlarged flow paths that have increased connectivity as a result of positive feedback between dissolution and flow focusing (Worthington et al., 2016). While the dividing line between conduits and fractures is somewhat arbitrary, often the conduits are defined as the flow paths that carry turbulent flow (White, 2002). The three porosity components differ in their ability to store and transmit water. Primary porosity provides much more storage than the conduit network, because of its large total volume, whereas conduits transmit the most water, because of their high permeability (Worthington, 1999). These different hydrologic characteristics create a strong scale-dependent hydraulic conductivity in karst aquifers. Hydraulic conductivity over short distances is controlled by the primary porosity and is thus relatively low. Hydraulic conductivity increases over intermediate distances as fractures become important and is greatest at aquifer scales where flow through conduits dominates (Halihan et al., 2000; Király, 1975; Worthington, 2009). In general, heterogenous media exhibit an increase of hydraulic conductivity with measurement scale, up to some cutoff scale where the medium is well-represented by an equivalent porous medium (Schulze-Makuch et al., 1999). However, the range of variation in hydraulic conductivity is largest in karstified media, as karst exhibits the largest cutoff scale (Schulze-Makuch et al., 1999), with individual aquifers having measured values of hydraulic conductivity ranging over more than eight orders of magnitude (Worthington, 2009).

The primary porosity within a carbonate rock is a function of its diagenetic history and whether the rock has undergone burial diagenesis, which reduces primary porosity. The terms eogenetic karst and telogenetic karst are used to distinguish karst that is developed within relatively young carbonates that have primarily undergone meteoric (eogenetic) diagenesis from karst developed in older carbonates that have experienced burial diagenesis (telogenetic) and re-exposure to the surface via erosion (Vacher and Mylroie, 2002; Choquette and Pray, 1970). Integrated karst flow networks develop most easily in rocks with relatively low primary porosity and relatively high fracture porosity (Palmer, 1991; White, 1969; Worthington, 2014). Such conditions focus flow through higher permeability fractures, increasing flow velocities and the depth to which undersaturated water can penetrate the rock, ultimately leading to breakthrough of dissolutionally enlarged pathways that connect inlets to outlets (Dreybrodt, 1990). Positive feedback further focuses the flow, whereby the most efficient flow paths receive the most flow and therefore grow most rapidly, diverting even more flow into these pathways and further

accelerating their growth (Ewers, 1982; Palmer, 1991; Siemers and Dreybrodt, 1998). The largest developing flow paths create troughs in the potentiometric surface, such that other competing pathways are drawn toward them, frequently producing a dendritic pattern like that found in surface stream networks. The overall conduit network geometry is strongly influenced by the nature of recharge to the aquifer and the locations of recharge and outlet points (Figure 2) (Palmer, 1991).

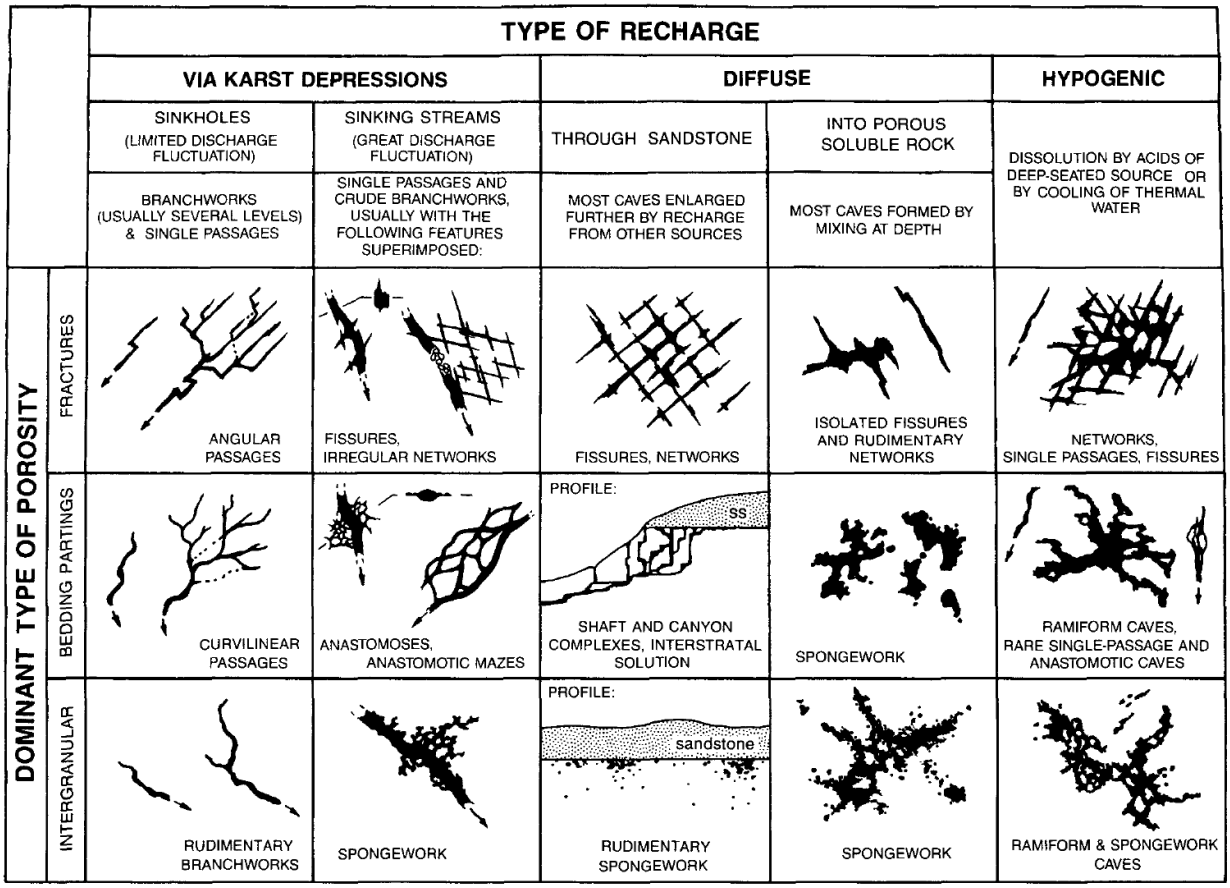

Figure 2. Relationship between recharge, dominant porosity, and the patterns of karst networks that develop (from Palmer, 1991).

Rocks with high primary porosity, as found in eogenetic karst, preferentially develop spongework caves (Palmer, 1991), which are often isolated voids that are not connected into an integrated conduit flow system (Vacher and Mylroie, 2002). Examples of such dissolutional voids include flank margin caves and "banana holes" that develop in carbonate island karst (Breithaupt et al., 2021; Mylroie and Carew, 1990; Vacher and Mylroie, 2002). In such settings, the locations of dissolutional voids may be controlled by zones of mixing (Mylroie and Carew, 1990) or by biological CO_2 production (Gulley et al., 2016, 2015). Consequently, voids frequently develop near the water table, where vadose zone CO_2 can boost dissolution rates (Gulley et al., 2014), or in zones of freshwater-saltwater mixing (Mylroie and Carew, 1990). While evolution of such voids produced by local mixing or CO_2 production may enhance local

hydraulic conductivity and focus porous media flow toward enlarging voids (Mylroie and Carew, 1990; Vacher and Mylroie, 2002), it is less common for these processes to develop regionally integrated conduit systems (Palmer, 1991). However, long-range conduit connectivity that does develop in eogenetic karst is commonly associated with sinking streams (Martin and Dean, 2001; Monroe, 1976), reversing springs (Gulley et al., 2011; Moore et al., 2010), or large recharge areas, as found in the Yucatan Peninsula of Mexico (Back et al., 1986) and on large carbonate islands (Larson and Mylroie, 2018).

The primary porosity of carbonate rocks also impacts the magnitude of water exchange between conduits and the porous matrix. The matrix component is often considered negligible in models of flow and transport in telogenetic karst aquifers (Peterson and Wicks, 2005). However, in eogenetic karst, with high matrix porosity, transient head conditions within conduits, combined with the relatively high permeability of the matrix, can produce substantial exchange flows between the conduits and matrix, analogous to hyporheic exchange within rivers (Martin and Dean, 2001). Such exchange flows may dampen the hydraulic response of karst aquifers, which are typically flashy (Florea and Vacher, 2006; Spellman et al., 2019). The loss of water from conduits into small intergranular matrix porosity increases surface areas available for dissolution reactions. In some cases, dissolution by exchange flow may be the primary factor driving evolution of connectivity within a karst aquifer (Gulley et al., 2011; Moore et al., 2010). Exchange flows are also important drivers of a variety of other biogeochemical reactions, in large part because of their control of redox condition as water equilibrated with atmospheric oxygen and elevated in dissolved organic carbon is injected into reducing water stored in matrix porosity (Brown et al., 2014; 2019; Flint et al., 2021). Such exchange flows can occur both between conduits and matrix and between rivers and the surrounding aquifer.

2.2 Sources of undersaturation and dissolution

In the classic conceptual model of karst development, calcite dissolution is driven by carbonic acid. Meteoric water dissolves CO_2 within the atmosphere and soil and carries this CO_2 downward into the rock, dissolving carbonate minerals along its way (Adams and Swinnerton, 1937). Karst developed by such processes is often referred to as epigene karst, indicating its close relationship to surface processes, in contrast to hypogene karst, which develops at depth. This classic conceptual model has been expanded in several ways, particularly as it relates to the sources of CO_2. In some karst settings, CO_2 concentrations are higher at depth than within the soil, suggesting CO_2 production deep within the vadose zone, perhaps as the result of the remineralization of particulate organic matter that has infiltrated to depth (Atkinson, 1977b; Mattey et al., 2016; Noronha et al., 2015;Wood, 1985).

In addition to carbonic acid, carbonate dissolution can be driven by a variety of other acids, with sulfuric and nitric acids being the most common. Sulfuric acid is widely cited as a source of dissolution in hypogenic speleogenesis (Egemeier, 1988; Engel et al., 2004), in marine carbonate sediments (Beaulieu et al., 2011; Torres et al., 2014), and in landscapes affected by acid rain (Shaughnessy et al., 2021). Sulfuric acid can be produced through fossil fuel combustion, especially coal (Irwin and Williams, 1988). Sulfuric acid is also produced where oxygen-rich air or water encounters reduced sulfur species such as pyrite in sedimentary rocks or H_2S produced by coupled microbial organic carbon oxidation and sulfate reduction. Carbonate dissolution can also occur by nitric acid produced during microbial nitrification or industrial processes. Nitric acid production has been enhanced by anthropogenic production of reactive

nitrogen species (Galloway, 1998; Galloway et al., 2008), for example by chemical fertilizer use in intensive agriculture and partial oxidation of atmospheric N_2 in internal combustion engines (Gandois et al., 2011; Perrin et al., 2008). Organic acids may also be important drivers of dissolution in some carbonate settings, although their concentrations are commonly lower than concentrations of sulfuric or nitric acids (Jones et al., 2015). High concentrations of organic acids have been suggested to cause rapid carbonate dissolution in a temperate rainforest setting (Allred, 2004; Groves and Hendrikson, 2011).

The source and type of acid causing carbonate dissolution is critical to global carbon cycling (Martin, 2017). Carbonate dissolution by carbonic acid is neutral with respect to long-term atmospheric CO_2 concentrations, because CO_2 consumed during weathering is balanced by CO_2 released during marine carbonate precipitation, with

CO_2 (atm) + H_2O (atm) + $CaCO_3$ (bedrock) → Ca^{2+} (river) + $2HCO_3^-$ (river) → $CaCO_3$ (marine) + CO_2 (atm) + H_2O (marine).

In contrast, dissolution of carbonates by sulfuric or nitric acids results in a net flux of CO_2 to the atmosphere (Martin, 2017), with

$$H_2SO_4 + 2CaCO_3 + H_2O \rightarrow CaCO_3 + CaSO_4 * 2H_2O + CO_2.$$

$$2HNO_3 + CaCO_3 \rightarrow Ca^{2+} + 2NO_3^- + CO_2 + H_2O$$

Considerable work over the last two decades has focused on hypogene speleogenesis, in which water undersaturated with respect to bedrock minerals forms at depth and is carried to the surface with regional groundwater flow (Klimchouk, 2007; Palmer, 1991). Undersaturated water may form through many mechanisms, including cooling of rising thermal waters, oxidation of reduced sulfur species, deep sources of CO2, and mixing of waters with different salinity or pCO_2. Dissolution deep within a karst aquifer may develop porosity that is disconnected from points of surface recharge, forming isolated porosity rather than regionally integrated flow networks. Alternatively, dissolution where deep and meteoric water mix may develop integrated flow networks if the pore spaces become linked. Karst conduit networks formed by hypogene processes typically develop complex mazes or ramiform passages, with less tendency toward the dendritic flow patterns common in epigene karst settings (Palmer, 1991). Porosity that develops in the deep subsurface may serve as a template for epigenetic karst processes when exhumation due to erosion brings that porosity closer to the surface (e.g., Tennyson et al., 2017).

2.3 Climate

Climatic factors impact the rates and forms of karst development (Lehmann, 1936). A theoretical relationship for the maximum possible rates of karst denudation (D_{max}) based on equilibrium carbonate chemistry (White, 1984) provides a first order estimate of the impact of climate factors on rates of carbonate denudation,

$$D_{\max} = \frac{100}{\rho}\left(\frac{K_c K_1 K_{CO2}}{K_2}\right)^{\frac{1}{3}} pCO2^{\frac{1}{3}}(P - E) \qquad (1)$$

where ρ is rock density, K_c, K_1, K_{CO2} and K_2 are temperature-dependent equilibrium constants of the carbonate system, pCO_2 is the partial pressure of CO_2, and $P - E$ is precipitation minus evapotranspiration. Equation 1 shows the three main contributors to climate-driven differences in carbonate denudation rates: 1) changes in the equilibrium constants with changing temperature, 2) differences in pCO_2, which are strongly related to temperature, and 3) water availability. Among these three factors, water availability plays the strongest role in producing global variation in chemical denudation rates (Ryb et al., 2014; Smith and Atkinson, 1976). Well-developed karst surface features are less common within hot and arid settings or cold settings where water is rarely present in a liquid state (Ford and Williams, 2007). When karst surface features are present in such settings, they are sometimes inherited from landscapes that developed in past conditions that were wetter.

As temperature increases, solubility of calcite decreases, largely because of the decreased solubility of CO_2. However, carbonate mineral dissolution rates increase with warmer temperatures (Plummer et al., 1978). Elevated dissolution rates decrease the time required to reach equilibrium within the CZ and thus faster kinetics lead to more dissolution within the near subsurface (Gabrovšek, 2009). In addition, soil pCO_2 increases with increased temperature as biological activity increases (Drake, 1980). These two competing effects, of decreasing solubility and increasing pCO_2 with increasing temperature, are thought to produce the observed boomerang shape between $Ca^{2+} + Mg^{2+}$ concentrations and temperature within world rivers, which suggests carbonate weathering intensity peaks around a temperature of 10° C (Gaillardet et al., 2019). While a substantial body of work examines fluxes of solutes from carbonate basins and uses these to estimate average denudation rates (e.g., Erlanger et al., 2021; Gunn, 1981; Lauritzen, 1990) the role of kinetics in partitioning dissolution within the subsurface remains an area for further study.

While, broadly speaking, the impacts of climate on karst processes are well-understood, many open questions remain. For example, polygonal or cockpit karst develops preferentially in the humid tropics, whereas doline karst is more typical of humid temperate regions, and the reason for this difference is unclear (Ford and Williams, 2007). Interactions between climate and biological processes may be an important driver in the evolution of these landscapes.2.4 Vadose zone gases and open vs. closed system weathering

Vadose zone gases, particularly CO_2 and O_2, play an important role in weathering processes (e.g., Brantley et al., 2013; Kim et al., 2017). These gases are derived from Earth's atmosphere as a primary source (Kim et al., 2017; Wood and Petraitis, 1984) and are often assumed to be transported by diffusion in the vadose zone. However, connectivity among solutionally enlarged fractures and larger conduits in karst systems enables advective gas flows. Advection is forced by density contrasts between surface and subsurface air, largely through temperature variations at daily and seasonal time scales (Covington, 2016; Covington and Perne, 2015; Sanchez-Cañete et al., 2011), that drive seasonal and diurnal changes in subsurface gas concentrations (Benavente et al., 2010; Gulley et al., 2014; Kowalczk and Froelich, 2010; Lang et al., 2017; Mattey et al., 2016; Milanolo and Gabrovšek, 2009; Sekhon et al., 2021; Spötl et al., 2005; Wong et al., 2011). These variations are likely to extend throughout the vadose zone, even where it may be thick because of deep groundwater tables (Benavente et al., 2010; Covington, 2016; Mattey et al., 2016). In some cases, soil and the shallow subsurface may be aerated from below rather than directly from the atmosphere (Faimon et al., 2020). The ventilation through

conduit systems, and the linked changes in vadose water chemical compositions and compositions at the water table, can thus provide controls on the spatial and temporal patterns of dissolution and precipitation of calcite (Covington et al., 2021; Covington and Vaughn, 2019; Gulley et al., 2014; Houillon et al., 2017; Spötl et al., 2005; Wong et al., 2011). Similar processes can impact CO_2 gas fluxes from, and carbonate weathering patterns within, the soil (Roland et al. 2013).

Weathering of carbonate minerals is often approximated as proceeding under open or closed system conditions with respect to a CO_2 gas phase. Under open system conditions, the solution is in contact with a large reservoir of CO_2 and evolves at fixed pCO_2, dissolving more CO_2 from the gas phase as CO_2 is consumed by carbonate dissolution. Under closed system conditions, the solution is isolated from the gas phase, and pCO_2 decreases as carbonate dissolution proceeds. Open and closed conditions are partly dictated by the water saturation state of the pore spaces, with complete water saturation producing closed conditions. Whether carbonate dissolution proceeds under open or closed conditions impacts both the rate of weathering processes (Buhmann & Dreybrodt, 1985a; Buhmann & Dreybrodt, 1985b) and trace element concentrations and isotopic compositions of dissolved species (Hendy, 1971; Stoll et al., 2022). A global study of spring water chemistry suggests that, on average, spring chemistry in carbonate regions is well-explained by weathering under conditions that are open to soil CO_2 (Romero-Mujalli et al., 2019).

The impact of carbonate weathering processes on the isotopic composition of speleothems was first investigated in the seminal work of Hendy (1971). Subsequent studies built on the model to discern the effects of prior calcite precipitation, which impacts trace element concentrations, and kinetic fractionation, which impacts stable isotope ratios, to confidently isolate climate signals from speleothems (e.g., Fohlmeister et al. 2011; Fohlmeister et al., 2020). The primary goal of these models is to illustrate the potential of speleothems to track changes in the climate. However, such studies also help us to better understand local hydrological processes dictating epikarst conditions, such as prior calcite precipitation, that are sensitive to open and closed system conditions and pore spaces in the CZ (Stoll et al., 2012). Recent work goes beyond the open/closed system framework and employs a reactive transport model to simulate carbonate weathering processes and gas transport in the carbonate CZ (Druhan et al. 2021; Oster et al., 2021). Such approaches provide a promising new avenue for future research on carbonate CZ processes. Lastly, to investigate the open versus closed system paradigm, variation in dead carbon fractionand Li isotopes of speleothems provide additional constraints on the relationship between climate and weathering. Dead carbon fraction in speleothems is primarily controlled by an uptick in limestone dissolution. This is typically indicative of closed system conditions during periods of increased hydrological activity (Griffiths et al., 2012; Bajo et al., 2017). Though enhanced decomposition of old, recalcitrant, carbon is another important source of dead carbon fraction (Rudzka et al., 2012; Noronha et al., 2015). Likewise, recent studies of Li isotopes within cave drip waters and analog experiments highlight the possibility of studying silicate weathering intensity using speleothem records (Day et al., 2021; Wilson et al., 2021).

2.5 Tectonic setting and base level

Tectonic uplift, sea level change, and other drivers of changes in base level provide important boundary conditions for the development of karst flow networks and the resulting landscapes. Karst conduit development is often focused near, or driven toward, the water table (Ford and Ewers, 1979). During periods of stable base level, karst conduit networks can preferentially develop within specific elevation ranges (Figures 3). Such cave levels are used to date phases of river incision using cosmogenic burial dating (Granger et al., 2001; Stock et al., 2005). Similarly, flat corrosion plains develop when the land surface approaches base level (Ford and Williams, 2007). In contrast, where rapid uplift occurs, the resulting high relief promotes the development of thick vadose zones, sometimes in excess of 2 km. In these cases, conduit development may be primarily vertical, along structural features such as faults, until water collects within subhorizontal conduits that drain the water laterally out of massifs into springs near base level (Audra et al., 2006; Turk et al., 2014; Klimchouk, 2019).

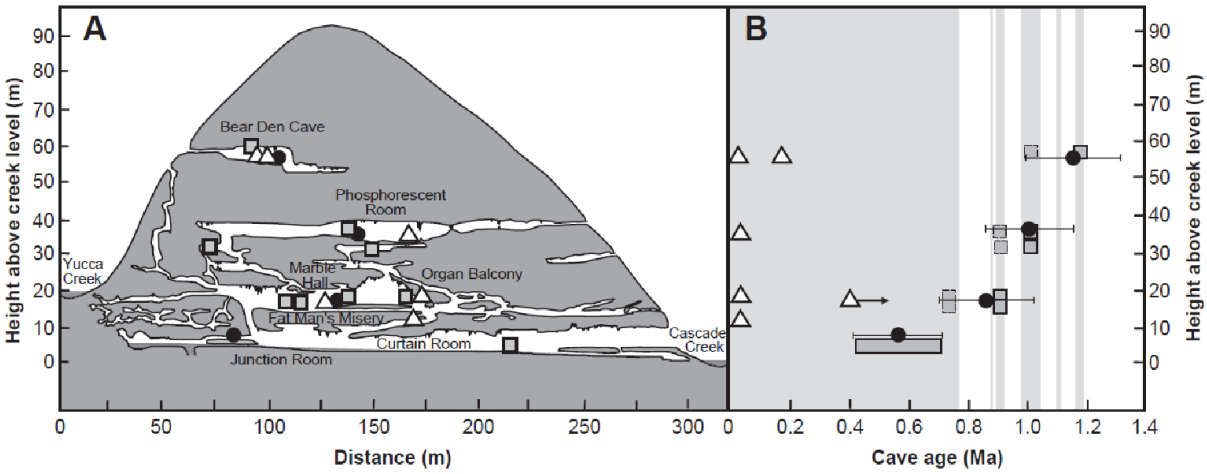

Figure 3. The development of horizontal cave levels in response to stream incision (from Stock et al., 2005). As the surface stream incised, new levels of cave passage were developed (A), rather than steepening of the existing channel, as would occur during a pulse of incision in a surface stream. Locations (A) and ages (B) of cave deposits are shown, including speleothem U-Th (white triangles), paleomagnetic (gray squares), and cosmogenic burial (black circles) samples. The cosmogenic burial ages of coarse sand and gravel are most indicative of the time when a cave passage was occupied by an active stream.

Uplift of carbonate platforms can also result from isostatic rebound caused by dissolution and the resulting reduction in platform density (Adams et al., 2010; Opdyke et al.,1984). In fold and thrust belts, the tendency for evaporites to act as planes of detachment frequently results in the formation of anticlines with evaporite cores (Davis and Engelder, 1985), and the buoyant effect of the evaporites may be an additional force contributing to uplift of the anticline (Lucha et al., 2012). The juxtaposition of evaporites below uplifted, fractured carbonate-rich rocks create ideal conditions for hypogene, sulfidic karst development, as in the Central Apennines, Italy (D'Angeli et al., 2019). In this setting, base level is controlled by river incision of the anticline, resulting in sulfidic springs that discharge in or near river valleys. Cycles of sea level rise and fall are important drivers of karst development in coastal settings, which are typical of most eogenetic karst. Voids that develop at sea-level low stands are subsequently flooded during sea level rise (Myroie and Carew, 1990; Smart et al., 2006; Gulley et al., 2013). Patterns of sea level

change can often be tracked within speleothem records (Bard et al. 2002; Roy & Mathews, 1972; Surić et al., 2009).

2.6 Relative importance of chemical vs. mechanical weathering processes

Landscapes that develop on carbonate bedrock are impacted by the types and rates of mechanical weathering and erosion. In landscapes where mechanical processes are more efficient than chemical processes, karst features will be less pronounced, even if subsurface karst flow networks are well-developed. The instantaneous rate of chemical erosion tends to be slower than the instantaneous rates of mechanical erosion processes such as bedrock abrasion, hillslope mass wasting, and glacial erosion. However, chemical erosion processes are often relatively continuous, with chemical denudation rates depending primarily on climate (White, 1984) and dissolution rates within streams showing relatively low variability over time (Covington et al., 2015). In contrast, mechanical erosion and mass transport processes are frequently episodic. Consequently, the most extensive karst landscapes develop in humid environments where nearly continuous chemical weathering outpaces episodic mechanical processes – a tortoise and hare analogy (Simms, 2004). In environments where mechanical weathering processes are particularly effective, karst surface features may fail to develop because of the rapid breakup and accumulation of weathered rock. One such example is alpine karst settings, where frost cracking can erase surface expressions of karst (Ford, 1971).

In mixed carbonate and non-carbonate terrains, carbonates can behave either as weaker rock layers, forming topographic lows, or as strong layers that form topographic highs (Simms, 2004; Ott et al., 2019). When chemical weathering rates outpace tectonic uplift, as might be the case in either humid environments or tectonically passive settings, then carbonates tend to erode more quickly and develop lows in the topography. However, when tectonic uplift outpaces chemical weathering, as in arid or rapidly uplifting environments, then the mechanical strength of carbonates may result in the formation of topographic highs (Ott et al., 2019).

The diversion of surface water, and therefore geomorphic work, into the subsurface in sinking streams can influence the efficiency of fluvial erosion processes. For example, karst sink points can stall the propagation of knickpoints, reducing rates at which stream profiles adjust to changes in tectonic forcing (Fabel et al., 1996). Ott et al., (2019) quantified both chemical and mechanical erosion rates in carbonates and non-carbonates in Crete, showing that mechanical erosion processes dominate, even in the carbonates, where chemical denudation accounts for ~40% of total erosion. Their results suggest that the much greater relief that develops in the carbonates results from loss of water into the subsurface and subsequent steepening of stream channels to enable mechanical erosion rates to keep pace with uplift.Chemical and physical processes can also interact, potentially enhancing or inhibiting each other. Experiments in subcritical cracking demonstrate unique fracture propagation behaviors in carbonates, which may relate to dissolution processes at fracture tips (Atkinson, 1984; Henry, 1978). In general, models and experiments suggest that acids can enhance fracture propagation rates in carbonate rocks (e.g., Hu & Hueckel, 2019). Roots are an important agent in mechanical breakup of rock, particularly in areas with thin regolith (Brantley et al., 2017). In carbonates, roots can take advantage of subsurface porosity generated by dissolution processes (Estrada-Medina et al., 2013), and they can also generate subsurface porosity through dissolution by root exudates or CO_2 generated by root respiration (Klappa, 1980; Rossinsky and Wanless, 1992), potentially enhancing root-driven rock fracturing. It has also been hypothesized that chemical and

mechanical erosion may enhance each other within stream channels (Covington, 2014; Covington & Perne, 2015), with chemical erosion potentially loosening grains that are then removed by mechanical processes (Emmanuel & Levenson, 2014), or with mechanical abrasion removing surface impurities to expose fresh weatherable carbonate minerals. Mechanical weathering processes can also inhibit chemical weathering processes. For example, buildup of fractured rock material on the surface, with high surface areas for reaction, may lead to saturation of meteoric water before it reaches unweathered bedrock. Similarly, high sediment loads within streams could armor the beds and inhibit dissolution except during periods of sediment mobility.

2.7 Biota

As in the CZ more generally, the activity and spatial architecture of carbonate CZ biological communities have important feedbacks to other CZ processes. Thanks to networks of large voids, the carbonate CZ is distinguished by the potential for macroscopic biota including fish, amphibians, and invertebrates to penetrate up to several km below the photic zone (Figure 4). Because both locomotion and passive transport in karst conduit networks are more constrained than at the surface, carbonate CZ biological communities often show a high degree of endemism. The resulting small population sizes leave carbonate CZ fauna especially vulnerable to extinction (Culver & Pipan, 2013).

Animal communities in the subsurface can be fed either by in situ microbial primary production or detrital dissolved and particulate organic carbon percolating downward from the surface soil. In some cases, sedimentation of particulate organic carbon in conduits creates a biological hot spot where CO_2 production from decomposition drives further carbonate dissolution (Covington et al., 2013; Gulley et al.,2016). In coastal karst landscapes where aquifers are density stratified and partially filled by anoxic seawater (i.e. anchialine), organic matter hot spots also facilitate H_2S production from microbial sulfate reduction. As water flows over the hot spot, H_2S is transported away and oxidized at redox interfaces elsewhere in the network, producing sulfuric acid that drives more carbonate dissolution. A striking example of this process can be observed in the Bahamas eogenetic karst. "Blue holes" (sinkholes) are extremely common in the landscape and collect surface vegetation, which is deposited at the bottom of the conduit in anoxic or dysoxic seawater. Tidal pumping exchanges low pH water between the blue hole and matrix porosity of these eogenetic karst features, enhancing dissolution reactions (Martin et al., 2012). Decomposition of the detrital plant material fuels intense H_2S production and, where the H_2S diffuses into the photic zone, associated blooms of sulfide-dependent photosynthetic bacteria thrive and fix additional carbon in the subsurface (Gonzalez et al., 2011, Haas et al., 2018).

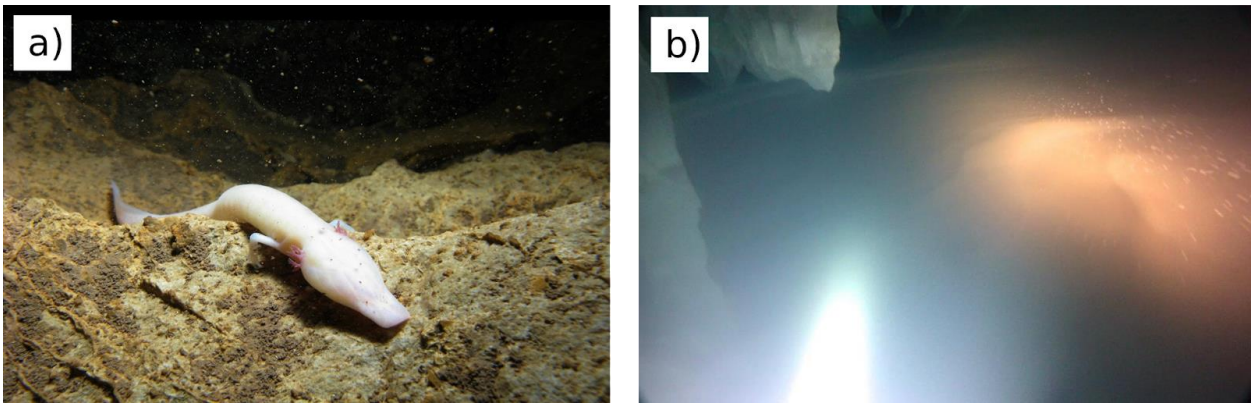

Figure 4. a) Proteus anguinus, an aquatic salamander found in the karst of the Dinaric Alps that is one of the largest cave adapted animals in the world (reaching up to 40 cm in length). Photo Gergő Balázs. b) A dense swarm of amphipods (Niphargus sp.) flee a diver exploring water-filled karst conduits ~400 m below land surface in the Frasassi cave system, Italy. Stable density stratification between sulfidic water and an overlying lense of oxic vadose water in the aquifer create enough chemical energy to support a rich food web based on microbial lithoautotrophy. Photo J. L. Macalady/A. Crocetti.

Vegetation on karst landscapes is affected by (1) rapid drainage and associated nutrient leaching due to thin soils and large bedrock pores, (2) phosphorous scarcity due to the low P content of carbonate bedrock and high phosphate complexation with abundant Ca^{2+} ions, (3) strong decimeter- to meter-scale spatial heterogeneity in topography, soil and hydrologic factors, and (4) slow soil formation due to limited silicate minerals with incongruent weathering to form clay minerals. The plant ecology of tropical and subtropical karst ecosystems has recently been reviewed in depth (Geekiyanage et al., 2019). Because water in thin karst soils is in short supply, plants growing on carbonate-dominated landscapes have adaptations for using alternative reservoirs of water, especially in dry seasons (Figure 5). Non-tree species often have particularly dense and extensive shallow root systems because they depend on soil water year-round (Ellsworth et al., 2015). Due to high bedrock porosity, water stored in the vadose zone (epikarst) represents a significant alternative to soil water for woody species that can penetrate into carbonate bedrock (e.g., Querejeta et al., 2007). Some woody species also have specialized, long roots that reach the water table (Deng et al., 2012; Swaffer et al., 2014). Adaptations for obtaining fog water (Fu et al., 2016), and a drought-deciduous strategy in which leaves are shed during dry seasons (Reich and Borchert, 1984; Wolfe and Jursar, 2015), have also been documented in plants growing in carbonate terrains.

Plant adaptations to obtain water resources in the carbonate CZ significantly alter the hydrologic balance at depths far below the soil zone, and therefore have feedbacks on weathering rates and nutrient and organic carbon transport out of the system that are different than in the silicate-dominated CZ (Huang et al., 2009; Dammeyer et al., 2016). Karst plant nutrient acquisition strategies may also differ significantly, with potential feedback to weathering rates. Plants growing on calcareous soils release organic acids from their roots in order to obtain phosphate (Ström et al., 2005). Subsequent microbial degradation of the organics further enhances CO_2 production near roots. In the presence of strong topographic heterogeneity leading to soil pockets in epikarst depressions, vegetation can reinforce CO_2-induced weathering hot spots in the landscape and thereby amplify dissolution along certain water flow paths. A well-studied example of vegetation-mediated positive weathering feedbacks can be seen in Big

Cypress National Preserve, South Florida, which is characterized by extensive spatial patterning (Dong et al., 2019a,b).

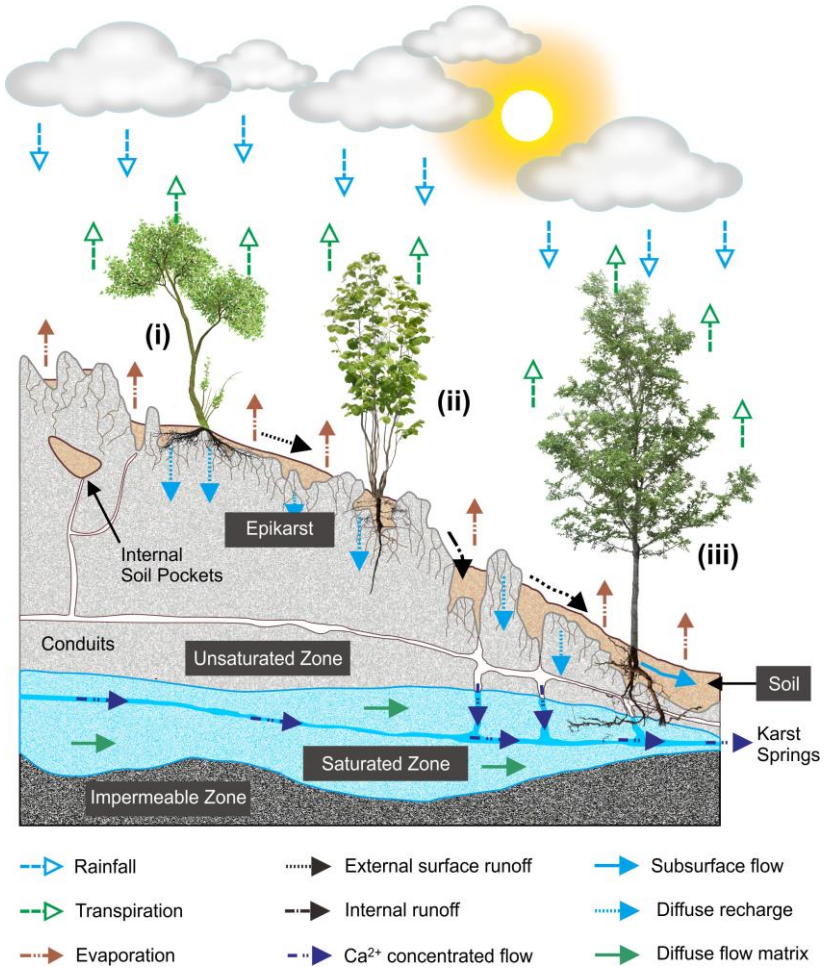

Figure 5. Water use strategies of karst plant species in a typical karst ecosystem during the dry season; (i) soil water dependent (species that predominantly take up soil water in both the dry and wet season), (ii) epikarst water dependent (species that use both soil and water stored in epikarst in both seasons and show a major shift to epikarst water when soil water is depleted during the dry season), and (iii) groundwater dependent (species that use groundwater in addition to soil and epikarst water and show a major shift to epikarst and groundwater when soil water is depleted during the dry season). Not illustrated here are (iv) fog water dependent plants, which use fog-derived water in addition to any of the above water sources, and (v) drought-deciduous (remain dormant by leaf shedding during the dry season). From Geekiyanage et al. (2019).

Plant roots and the microbial communities they support, including mycorrhizae, saprotrophic fungi, bacteria, and archaea have long been recognized as drivers of chemical weathering and the global carbon cycle (Beerling, 1998; Berner, 1992; Brantley et al., 2017a). Plant growth elevates soil pCO_2 and increases dissolved inorganic carbon (DIC) fluxes (Andrews and Schlesinger, 2001; Berner, 1997). Rooting systems (e.g., grass-, shrub- and woodlands) govern the distribution of soil carbon (both organic and inorganic), microbial biomass, and soil respiration (Billings et al., 2018; Drever, 1994; Jackson et al., 1996). For example, relatively

deep root distributions in shrublands compared to grasslands lead to deeper soil carbon profiles (Jackson et al., 1996; Jobbágy and Jackson, 2000), which elevate CO_2 and therefore weathering at depth. The work described here was carried out almost exclusively at sites where the CZ is dominated by silicate minerals. Only recently have similar ideas been applied to carbonate terrains, particularly in connection with studies of land-use changes.

Changing land cover has been invoked to explain changes in carbonate weathering processes. In carbonate terrains, carbon sequestration has been found to be optimized in grasslands as compared to shrub, managed crop, soil denuded of vegetation, or bare rock dominated landscapes (Zeng et al., 2017). This optimization results from greater pCO_2 and greater depths of water penetration in grasslands as compared to other land cover types. Woody vegetation encroachment into grasslands underlain by carbonate systems causes shifts in flow paths, groundwater solute concentration, and the timing of solute delivery to streams as inferred from reactive transport models and observed changes in stream and groundwater chemical compositions (Sullivan et al., 2019), with deep root systems regulating how much CO_2 is transported downward to the deeper carbonate-rich zone (Wen et al., 2020). Changes in pCO2 as a response to vegetation and landscapes can also be discerned through ^{13}C variability in speleothems. Lechleitner et al. (2021) show that an increase in soil gas pCO_2 is recorded in speleothem carbon isotope ($\delta^{13}C_{spel}$), which may retain information on soil respiration. Similarly, Stoll et al. (2022), attribute trends in $\delta^{13}C_{spel}$ to soil gas and bedrock dissolution. They propose that higher temperatures increase vegetation productivity, thereby increasing soil CO2 production, which leads to more negative $\delta^{13}C$ in speleothems.

Bedrock type can control plant productivity through influencing the available nutrients and physical regolith structure (Hahm et al., 2014). Data from carbonate settings suggest that silicate percentage is negatively correlated with the rate of water drainage from regolith and positively correlated with primary productivity (Jiang et al., 2020). It is hypothesized that preferential drainage features are better developed within carbonate-rich rocks and that this leads to both water and regolith loss into the subsurface, reducing water availability during dry periods. Similarly, a global study of relationships between rock type and biodiversity in erosional landscapes demonstrates that regions rich in carbonates have less vegetation and lower animal richness (Ott 2020).

2.8 Humans and the carbonate CZ

Human activity over millennia is intimately tied to use of karst landscapes for agricultural purposes, water resources, and cultural traditions (Quine et al., 2017; Stevanović, 2018; Moyes et al., 2009). The study of human evolution is rooted in investigating hominin bearing fossils discovered in caves (Mijares et al., 2010; Zanoli et al., 2022; Pickering et al., 2011; Sutikna et al., 2016) as well as cave art (Brumm et al., 2021; Valladas et al., 2001). Excavations of fossils in cave deposits continue to be a crucial tool in piecing together the history of human evolution. However, destruction of cave sites through cave infilling because of construction, and visitors destroying artifacts, threaten these prehistoric records. Interdisciplinary research between social scientists, geographers, archaeologists, and earth scientists is required to better constrain the relationships between humans and their interactions with karst landscapes. Human activity through the Anthropocene is negatively impacting the karst landscape (Long et al., 2021; Beach

et al., 2015). This delicate environment is susceptible to soil degradation, sinkhole development, groundwater contamination, and depletion in groundwater levels. Globally, many regions with carbonate aquifers are predicted to experience lower precipitation and higher temperatures, reducing recharge and stressing available water resources (Hartmann et al., 2014). Similar to geochemical processes, environmental impacts can occur more rapidly in karst and carbonate systems. The consequences of human activities in the carbonate CZ are highlighted below to draw attention to the vulnerability of karst that requires further research.

Karst uplands are vulnerable to runaway degradation if trees are removed. In the absence of forest vegetation protecting thin soils, rapid erosion into exposed karst fissures culminates in the creation of rocky deserts where forest vegetation can no longer get a foothold. Rocky desertification has occurred in significant areas of Mediterranean Europe (e.g., the Dinaric Karst), on islands such as Haiti and Barbados in the Caribbean, and especially and most recently in southwestern China (Jiang et al., 2014; Green et al., 2019). Over the past 50 years, a variety of human activities have played a substantial role in the expansion of rocky deserts in China including fuelwood collection, development of housing and tourism, slope cultivation, and animal grazing (Zhao and Hou, 2019). Populations are impacted as farmable land can switch from soil covered to denuded relatively rapidly (Zhao et al., 2020).

Sinkholes are one of the costliest hazards in karst regions, when collapse of underground voids intersects with human land use (Gutiérrez et al., 2014). Anthropogenic activities can accelerate sinkhole development, through lowering of the water table, diversion of recharge into karst depressions, or creation of water table fluctuations (e.g., Newton, 1987; Parise et al., 2015; Waltham, 2008; Yizhaq et al., 2017). Consequently, sinkhole hazards are closely linked to human activities through both water extraction and land development. These hazards may be exacerbated with future climate change as carbonate regions experience lower precipitation and more extreme precipitation events, further stressing water resources and creating higher runoff and larger water table variation.

Carbonate aquifers are particularly vulnerable to contamination (e.g., Hartmann et al., 2021; White et al., 2016), and because of enlarged passages a wider range of contaminants such as pathogens, contaminants sorbed to particles, and trash need to be considered (Ford and Williams, 2007; Vesper and White, 2003). Microplastics have recently been identified in karst systems but little is known of their sources, fate and impacts (Panno et al., 2019; Balestra and Bellopede, 2022). Predicting contaminant transport pathways is complicated by mixing of fast and slow flow paths, reflecting a need for an improved understanding of flow components and storage (Tobin et al., 2021). Furthermore, karst systems are more vulnerable to changing climate regimes, which increase or decrease precipitation inputs and may require special protection measures such as larger stormwater control structures (Veni et al., 2001). Recharge into karst aquifers can be enhanced because of heterogeneity, and a model of karst aquifer recharge suggests that heterogeneity influences recharge sensitivity to climate change, in some cases reducing sensitivity, and in some cases increasing it (Hartmann et al., 2017). Therefore, the heterogeneity of karst needs to be explicitly accounted for within water management strategies that consider impacts from climate change.

3 The carbonate-silicate spectrum

Due to fundamental differences in the properties of silicate and carbonate mineral groups, the percentage and spatial distribution of carbonate minerals within parent rocks drive important differences in the processes and architectures that develop as the CZ evolves. As a conceptual framework, we will consider a silicate-carbonate spectrum (Figure 6), with endmember landscapes completely dominated by either carbonate or silicate minerals. This framework provides a link between prior CZ studies and synthesis studies yet to be carried out in both carbonate and silicate-dominated sites along the spectrum. Understanding how CZ dynamics and processes change along this spectrum is a crucial next step towards integrating carbonate landscapes into existing knowledge of the CZ. We argue that studying the carbonate CZ will also contribute to new understanding of silicate settings by comparison.

3.1 Silicate-carbonate mineral mixtures and distributions in the CZ

Within Earth's CZ, silicate and carbonate minerals occur in mixtures across a range of scales, from the grain scale to stratigraphic scales (Figure 6). At the grain scale, all carbonate rocks contain some percentage of non-carbonate minerals, with common constituents including clays and slowly weathering silicate minerals such as quartz and feldspars (Ford and Williams, 2007). Silicate mineral fractions of carbonate rocks often take the form of sand- or silt-size quartz grains, or nodules or beds of authigenic chert (Figure 7a). These minerals may remain as lag deposits as the carbonate minerals are dissolved (Figure 7b-c). Similarly, many siliciclastic rocks contain some fraction of carbonate minerals, often in the form of a cement between grains. Carbonate-cemented sandstones, or impure carbonates, can form caves and karst landforms through the process of phantomization (Dubois et al., 2014; Häuselmann and Tognini, 2005; Kůrková et al., 2019), whereby preferential dissolution of the cement disintegrates the rock and then the remaining loose sand grains are removed physically by piping (Figure 7d). Counterintuitively, the effectiveness of the phantomization process is only weakly dependent on carbonate percentage, and instead disintegration is largely controlled by the grain-size and texture of the silicate component (Kůrková et al., 2019). This observation suggests that the change of landforms and CZ architecture along the carbonate-silicate spectrum depends on variables other than just the carbonate fraction of the lithology, such as how the mineral groups are distributed at the grain scale.

In addition to mixtures at the grain scale, silicate and carbonate rocks occur as relatively pure beds in layered stratigraphy (Figure 6). Terrains composed largely of carbonates may contain continuous beds of non-carbonates such as chert or shale. The layering creates heterogeneities in porosity and permeability with silicate mineral layers often less permeable than carbonate layers. The contrasts in permeability can create perched water tables and zones of focused conduit development in the carbonate layers (Figure 7e), while the impermeable silicate mineral layers tend to impede vertical flow of water. Sometimes carbonates are thinly interbedded with impure carbonates, shales, or other non-carbonate rocks, creating a landscape referred to as merokarst (Cvijic, 1925). Merokarst typically displays little surface topographical

expression of karst but may still behave hydrologically like a karst system (Brookfield et al., 2017; Macpherson and Sullivan, 2019a; Sullivan et al. 2020).

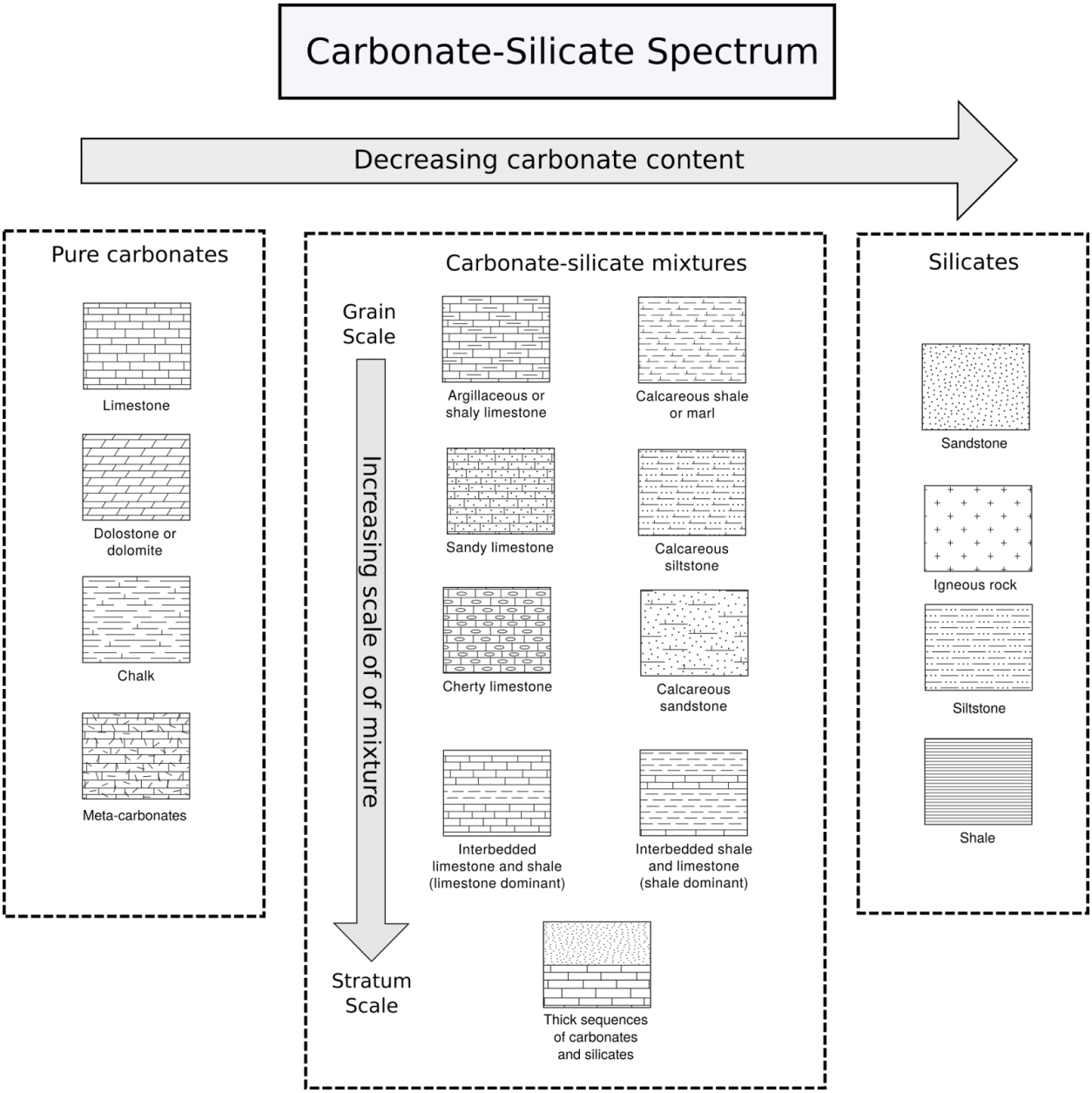

Figure 6. The carbonate-silicate spectrum. In addition to end-member cases of pure carbonate and silicate rocks, carbonates and silicates commonly occur as mixtures. Both the carbonate percentage and the scale over which the two mineral types mix are crucial parameters that will influence critical zone structure and evolution.

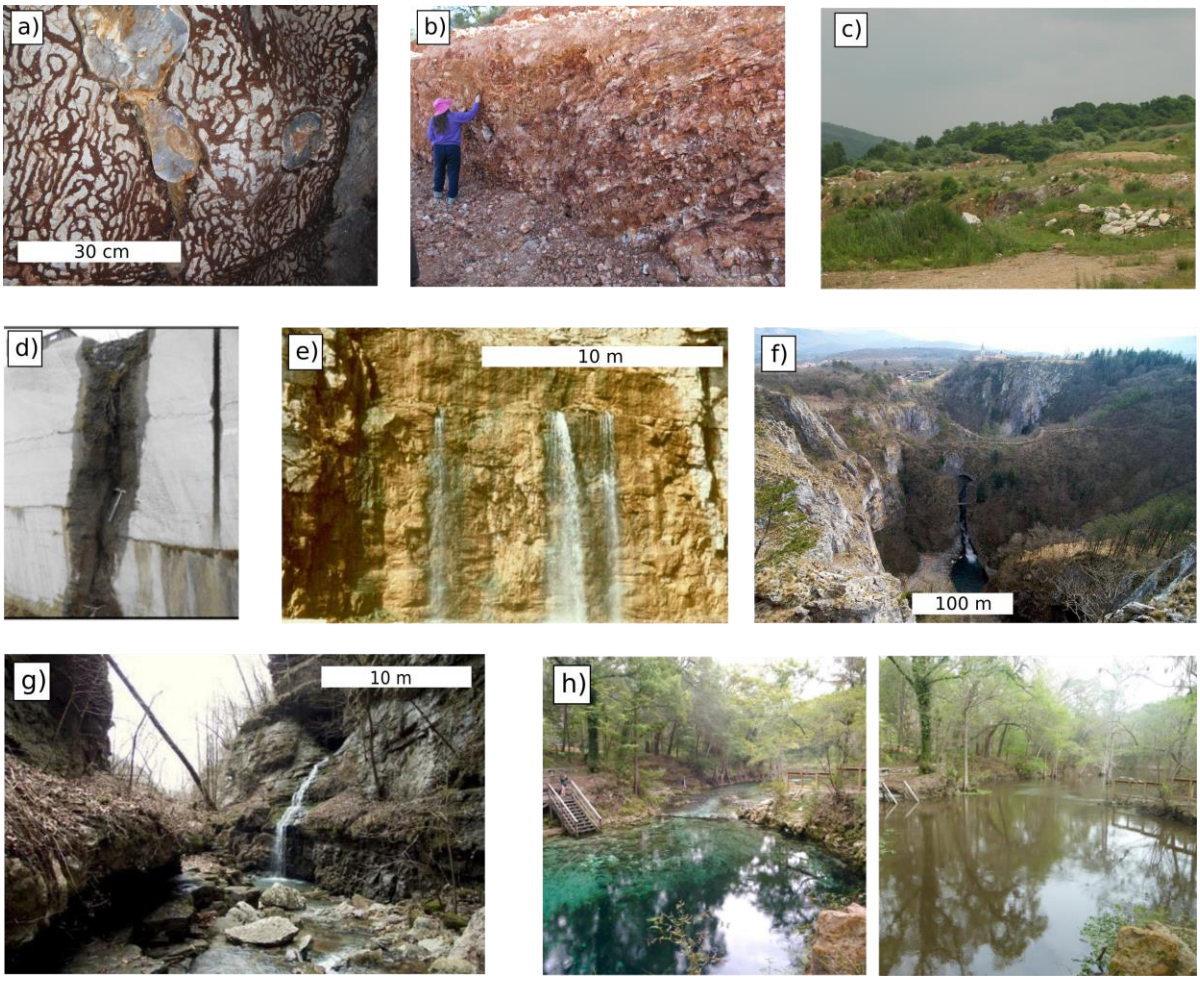

Figure 7. Features illustrating aspects of the carbonate-silicate spectrum. a) Differential weathering of chert nodules within micritic limestone in Grotta Sulfurea, Frasassi, Italy. The cave walls are colonized by microbial biofilms (biovermiculations) that prefer the carbonate to the silicate surface, b) A thick regolith layer of chert and clay left behind after dissolution of the Boone Limestone, Arkansas, c) Weathering residuum drapes crystalline dolomite of the Cambrian Ledger Formation in Pennsylvania, d) Ghost-rock karstification (phantomization), whereby weathering residuum is left behind within solutionally altered preferential flow paths, near Soignies, Belgium (from Dubois et al., 2014), e) Water emerges from a bedding plane on top of a chert layer within a carbonate rock, Arkansas, f) The Reka River in the classical karst region of Slovenia sinks after flowing from flysch onto limestone, creating two large 160-m deep collapse dolines and the upper entrance to Škocjan Caves, g) A perched spring creates a waterfall at the contact where a limestone unit overlies a sandstone, Indian Creek, Arkansas, h) Madison Blue Spring, Florida, an estavelle, which functions as a spring in baseflow conditions (left) and reverses flow direction to receive organic-rich water from the Withlacoochee River during flood events (right).

Thick carbonate layers may be juxtaposed laterally with non-carbonate rocks. Contacts between carbonates and non-carbonates that are exposed at the surface typically form regions of focused interaction between surface and subsurface hydrological, geomorphological, and biological processes (Atkinson, 1977a; Brucker et al., 1972; Gulley et al., 2013; Khadka et al.,

2014; Martin and Dean, 1999; Palmer, 2001). When surface water flows from non-carbonate onto carbonate rocks, sinking streams, blind valleys, sinkholes, and open cave shafts often develop (Figure 7f). These vertical conduits capture surface runoff and route it into the subsurface. Likewise, springs are common features at contacts where confining non-carbonate rocks underlie carbonate rocks (Figure 7g). Such underlying confining units may produce a stratigraphically determined base level for the development of karst flow systems. Springs are also common where the water table intersects the land surface because erosion has removed silicate rocks and exposed high permeability zones in the underlying carbonates. Contact zones can also host estavelles (Figure 7h), features that alternate between acting as springs and sinks depending on the relative elevations of the water table and the surface water that receives spring discharge. When the surface water level at the spring rises above the hydraulic head at an estavelle, surface water may intrude into the spring, which can aid dissolution (Gulley et al., 2011) and alter concentrations of redox sensitive solutes (Brown et al., 2019).

3.2 Differences between carbonate and silicate settings

CZ architecture and dynamics differ substantially between settings that are dominated by either carbonates or silicates. Here we examine these differences, contrasting the end-member cases. Less is known about how these differences emerge along the carbonate-silicate spectrum, the parameters that control these changes, and whether changes occur smoothly with these parameters or exhibit non-linear, threshold responses. Understanding how the CZ varies along the entire carbonate-silicate spectrum is an important area for future research.

3.2.1 How deep is the CZ?

The dissolutional enhancement of permeability, and the resulting high flow velocities (Worthington et al., 2016), produce rapid advection of solutes into the subsurface. After development of preferential flow paths, substantial changes in flow and chemistry can be expected deep within and throughout the carbonate CZ over short time periods, such as individual storm events. Such variability is expected both within larger dissolutional conduits (e.g., Ashton, 1966; Birk et al., 2006; Brown et al., 2014; Covington et al., 2012; Groves and Meiman, 2005; Gulley et al., 2011; Liu et al., 2004; Vesper and White, 2004) and within smaller dissolutionally enlarged fractures and the epikarst (Kogovšek and Petrič, 2012; Liu et al., 2007; Miorandi et al., 2010; Musgrove and Banner, 2004; Tooth and Fairchild, 2003). Consequently, within the carbonate CZ, surface-like geochemical conditions can occur at substantial depth and at long distances from locations of point recharge. These changes deep within the carbonate CZ differ from the commonly assumed base of the silicate CZ as the depth where regolith formation begins (Figure 8). Thus, an important consideration in contrasting Earth's CZ in endmember carbonate and silicate settings lies in the definition of the CZ itself, specifically, its lower boundary, and the lower boundary's relationship with the mineralogical makeup of the CZ and active circulation of water (Condon et al., 2020).

Riebe et al. (2017) review possible criteria for defining the base of the CZ. Ultimately, they settle on an equilibrium-based definition, that is, the base of the CZ is the depth in the subsurface at which meteoric water and Earth materials are at chemical equilibrium. Although they do not explain why, they also note that a different definition may be needed for carbonate settings. We see two ways in which the equilibrium definition might be problematic in carbonates. First, given that active dissolution of calcite by meteoric water can occur at great

depths, up to thousands of meters (Klimchouk, 2019), the lower boundary using this definition can be quite deep, leading to a picture of the CZ that differs substantially from the typical hillslope catena (Figure 8). However, given that deep karst conduits can provide important controls on the fluxes of water, gas, and sediment through the CZ, it seems that a holistic understanding of the carbonate CZ requires an incorporation of coupling between the near and deep subsurface. Therefore, the extreme depth of carbonate dissolution illustrates a meaningful difference in the dynamics and processes that occur in carbonate and silicate settings.

Perhaps ironically, the second potential problem that we can see with the equilibrium definition of the base of the carbonate CZ is that, due to rapid kinetics, meteoric water equilibrates quickly with carbonates. Consequently, water may be effectively saturated with calcite in the near subsurface, ending further chemical weathering. That is, the equilibrium definition may specify too shallow a depth of the CZ, with a bottom boundary that is above depths in which additional CZ processes occur. In fact, these two problems can be seen as opposite sides of the same coin. They both result from the non-planar nature of the weathering front within carbonates (Phillips et al., 2019). Although meteoric water often comes close to equilibrium with calcite in the near subsurface, non-linear kinetics reduce dissolution rates as water nears equilibrium with carbonate minerals, enabling undersaturated water to penetrate deep into the subsurface (Dreybrodt, 1990; Palmer, 1991). Even in the absence of such non-linear kinetics, flow fingering or "wormhole" development can drive undersaturated water deep into dissolving fractures (Szymczak and Ladd, 2011, 2012). Additionally, dissolutional capacity can be added to alter equilibrium conditions in the deep subsurface by many processes. These processes include CO_2 production (Atkinson, 1977b; Benavente et al., 2010; Gulley et al., 2015; Mattey et al., 2016), mixing of surface-derived meteoric water with water containing H_2S (Davis, 1980; Egemeier, 1987; Hill, 1990; Jagnow et al., 2000; Palmer, 1991; Martin, 2017), mixing of water with different partial pressures of CO_2 (Bögli, 1964; Wigley and Plummer, 1976), or mixing with salt water (Back et al., 1986; Mylroie and Carew, 1990; Plummer, 1975). Each of these processes may alter the equilibrium conditions deep within the CZ.

Despite potential difficulties outlined above, we think that an equilibrium-based definition of the lower boundary of the CZ in carbonates is a reasonable starting point. A working definition of the base of the CZ in carbonate settings would then be, "The depth below which there is no measurable dissolution of carbonate minerals by meteoric water." This definition comes with the caveats that: 1) much of the water between the surface and the base of the CZ will be near equilibrium with respect to carbonate minerals, even though it is within the CZ, and 2) some of the dissolution will be driven by subsurface acid production and/or mixing of meteoric water with deeper water. Perhaps the most difficult delineation to make is between dissolution processes that are driven by proximity to Earth's surface and those which can occur at great depth from rising thermal waters, H_2S-rich fluids, or volcanic production of CO_2. While many of these deeper processes may create a template for further permeability development by near-surface processes as rocks are exhumed, they can be considered as initial conditions for CZ development, much like the initial mineralogy, fabric, and structures of the exhumed rock layers, rather than an integral component of CZ processes. Here, we propose that dissolution processes that should be considered to define the bottom boundary of the CZ are those that produce feedback with the near-surface hydrological, geomorphological and biogeochemical processes, such that the dissolution processes both influence and are influenced by the flow of meteoric water.

3.2.2 The Conveyor model and CZ architecture

We use a conceptual model central to understanding CZ evolution within silicate terrains – the CZ conveyor (see e.g., Riebe et al., 2017) – to explore differences between the CZ in carbonate and silicate endmembers. Within the CZ conveyor model (Figure 8a), minerals are brought upward toward Earth's surface via erosion, exposing them to physical, chemical, and biological gradients. These gradients drive incongruent weathering that transforms bedrock into regolith that is transported down hillslopes toward stream channels. Through the migration of knickpoints, the stream channel network communicates erosion rate changes driven by tectonics or isostasy upward to the hillslopes. As channels at the base of hillslopes experience a change in erosion rate, hillslope topography and downslope transport of regolith adjust to accommodate the change. This system reaches topographic equilibrium when fluxes of fresh rock into the CZ are balanced by fluxes of solutes and sediments out of the channel network, resulting in a steady soil and regolith thickness. This conceptual model, in various forms, is ubiquitous throughout CZ studies (Amundson et al., 2007; Anderson et al., 2013, 2002; Brantley et al., 2017a; Heimsath et al., 2020; Hilley et al., 2010; Lebedeva et al., 2010; Patton et al., 2018; Rempe and Dietrich, 2014; Riebe et al., 2017).

Arguably the most fundamental difference between the weathering of silicates and carbonates is that carbonate minerals weather congruently, while silicate minerals weather incongruently. Incongruent weathering provides a key aspect of the conveyor model, whereby only a portion of the rock is removed in solution and the remaining sediment is transported to channels via hillslope processes (Figure 8a). This model thus predicts dynamic adjustment of soil and regolith thickness, producing negative feedback that drives soil production and rock lowering toward the average landscape erosion rate. When erosion rates increase, the down cutting of channels steepens the hillslopes and thins the soils, accelerating soil production. When erosion rates decrease, reduction in the rate of stream incision leads to reduction in hillslope relief, accumulation of soil, and reduction of weathering rates as soil thickens (Heimsath et al., 1997).

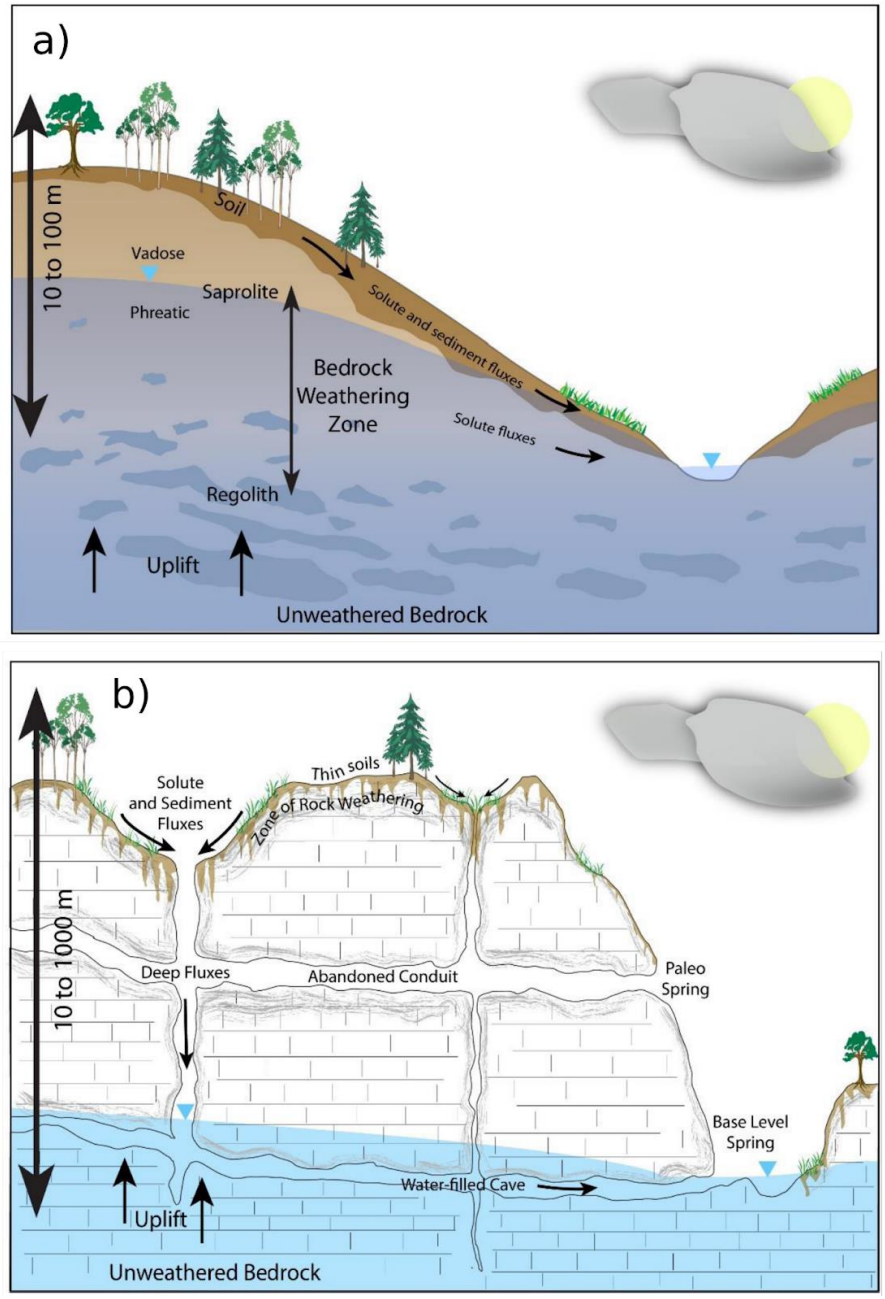

Figure 8. Carbonates and the conveyor model of the CZ. a) The conveyor model of the CZ, whereby uplift brings unweathered bedrock toward the surface. Weathering processes convert the bedrock into regolith and soil. Gravity transports sediment down the hillslopes, and stream channels carry away the solutes and sediments that are the byproducts of weathering. Communication between the hillslopes and channel network enables equilibration of the landscape to a rate of steady base level fall. b) Conceptual model of a well-developed karst in a carbonate setting. Surface drainage is limited. Congruent weathering of the carbonate rock leaves behind a thin soil. Much of the residuum from carbonate weathering may be routed through internally drained basins into the karst conduit network, potentially disconnecting hillslope response from changes in the rate of base level fall. Karst systems often respond to base level fall through the development of additional levels of conduits. Rapid carbonate weathering can occur deep within the subsurface in the vicinity of conduits and fractures.

Unlike silicate minerals, however, congruent weathering of carbonate minerals leaves only minor amounts of insoluble residue and therefore little soil or regolith (Figure 8b). Soils in carbonate terrains may develop largely from aeolian dust deposition (Macpherson and Sullivan, 2019b), and soil thickness may depend more on the carbonate purity or dust delivery rate rather than erosion rates such as in silicate terrains (Green et al., 2019; Moore et al., 2017). Additional differences result from the greater solubility and faster reaction kinetics of carbonate than silicate minerals (Plummer et al., 1979; Svensson and Dreybrodt, 1992). Carbonate dissolution is sufficiently fast that in some cases, chemical denudation rates can outpace mechanical denudation processes (Simms, 2004), such that solute fluxes may represent the majority of the seaward flux of weathering products.

Feedback mechanisms between soil development and denudation may be weakened, or even decoupled, within pure carbonate settings, particularly if the rate of soil development is controlled by allochthonous dust input. Carbonate denudation also may be controlled more by water availability and pH, rather than by topography or soil thickness as in silicate terrains (Gabrovšek, 2009; Gombert, 2002; Ryb et al., 2014; White, 1984). The weakening of feedback between soil formation rates and denudation rates may inhibit the approach to topographic equilibrium or at least increase the equilibration timescale. However, equilibrium landscape configurations that are entirely internal (autogenic) are also possible. For example, biogeomorphic feedbacks between soil thickness, CO_2 production, and weathering rates can produce equilibrium landscapes within low relief carbonate settings, where the water table is near the surface such as Big Cypress Swamp in southern Florida (Cohen et al., 2011; Dong et al., 2019a, 2019b). Here, modeling and field data suggest that initial development of a karst depression leads to the accumulation of both soil and colonization by rooting plants. As soil thickens, water becomes more available, and root respiration increases, increasing the pCO_2 at the rock surface and accelerating rates of rock weathering and depression growth. However, once sufficiently thick, soil cover inhibits the delivery of CO_2 to the rock surface. Ultimately, these feedbacks can produce a patterned equilibrium landscape that depends on internal controls rather than external erosional or tectonic forcing. Within the conveyor belt conceptual model for the silicate CZ, weathering occurs along planar fronts that are subparallel to the land surface (Figure 8a). In karstic carbonate terrains, weathering is focused along high permeability zones that create heterogeneous and irregular weathering patterns (Figure 8b) that are rarely subparallel to the surface (Phillips et al., 2019; Williams, 1985). Active weathering thus spans a range of depths, from exposed rock at the surface to rock that is hundreds, or even thousands, of meters below the surface (Audra et al., 2007; Klimchouk, 2019). The upper zone of weathering, often called the epikarst, typically has a higher degree of irregularity than the surface topography (Figure 9). This irregularity can grow over time through positive feedback resulting from flow-focusing (Klimchouk, 2004; Williams, 2008a, 1985) and generation of soil CO_2 that enhances shallow dissolution (Dong et al., 2019a; Gulley et al., 2015). The control of spatial weathering patterns in the subsurface of karst by geological structures and hydrological boundary conditions (Palmer, 1991), rather than soil properties or topography, indicates that models of carbonate CZ evolution will need to incorporate heterogeneity explicitly, as has been done in models of cave development (Dreybrodt, 1990; Gabrovšek and Dreybrodt, 2001; Groves and Howard, 1994; Hanna and Rajaram, 1998). These heterogeneities are missing from the lateral homogeneity of the conveyor belt model of the silicate CZ (Figure 8a).

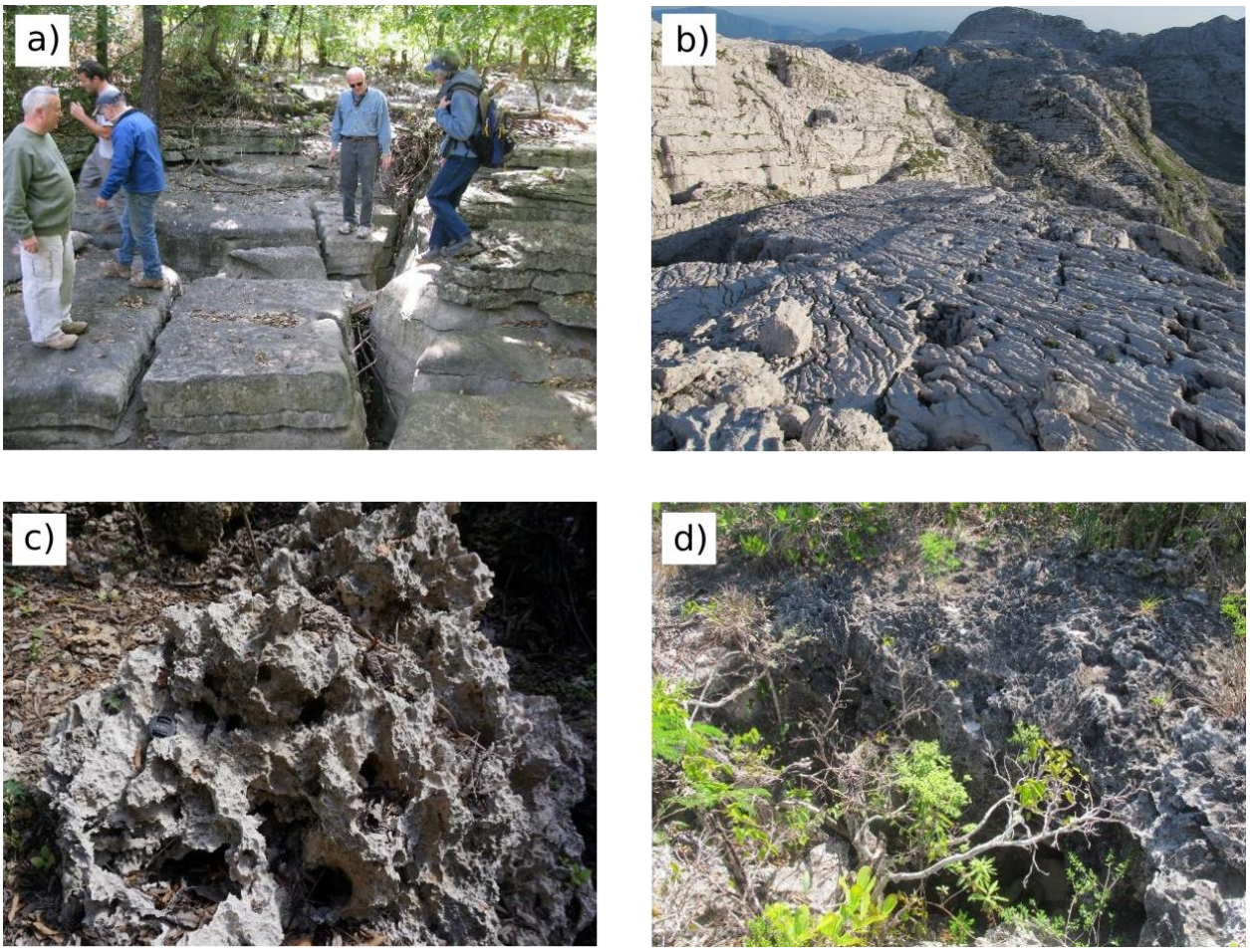

Figure 9. Weathering surfaces in carbonate terrains. a) Weathering along orthogonal joints in the St Joe Limestone in northern Arkansas. Floodwaters from a dam spillway have eroded the soil and exposed the weathering epikarst. b) Karren and epikarst surface on Dachstein Limestone on Mt. Kanin, Slovenia. c) Intense solutional weathering on an exposed piece of young, porous carbonate in Zanzibar. d) Thin soil and vegetation drape the weathering surface of young carbonates on San Salvador Island, Bahamas. In the center of the photo is the entrance of a 7-meter-deep solution shaft.

The focus of dissolution along high permeability zones in carbonate terrains causes an additional breakdown of the coupling between tectonic uplift and erosion rates found in the conveyor model. In the conveyor model, surface streams transport the sediment and solutes delivered to them by hillslopes (Figure 8a), enabling landscape-wide equilibration of erosion to uplift. However, surface streams are largely absent within a mature karst terrain, as all runoff and sediment generated near the land surface is diverted into the karst conduit system through closed basins (dolines or sinkholes) (Figures 8b, 10) (Ford and Williams, 2007). Thus, if the conveyor model of the CZ is transposed from silicate to carbonate terrains, dolines would represent hillslopes, and conduits would represent stream channels (Figure 8b). Even with relatively little relief (tens of meters), the hillslopes of dolines may be decoupled from base level, as dolines typically feed water and sediment vertically into the subsurface along solutionally enlarged

fractures and conduits (Brucker et al., 1972; Klimchouk, 2004; Palmer, 1991; Williams, 1985). Therefore, many of the "hillslopes" of karst terrains terminate at the tops of vertical subsurface channels.

Even in the case of dolines feeding into subhorizontal conduits, changes at base level may not propagate through karst conduit networks as they do through surface channel networks. First, the geometry of karst conduits, including the profiles of the streams within them, are often controlled by structural heterogeneities in the rock, such as bedding partings and fractures (Filipponi et al., 2009; Lowe and Gunn, 1997; Palmer, 1991). Therefore, the initial profiles of streams within karst conduits may be far from the equivalent equilibrium channel morphologies (e.g., slope-discharge relationships) that would be expected within surface stream channels. Second, under conditions of rapid base level change, karst systems often respond by the development of new levels and abandonment of old cave channels (Figures 3 and 8b) (Audra et al., 2007; Gabrovšek et al., 2014; Granger et al., 2001; Stock et al., 2005; Wagner et al., 2011), rather than through the propagation of knickpoints. Similar shifts in cave development in coastal carbonate settings result from variations in sea level (Florea et al., 2007; Gulley et al., 2013). The development of new levels within karst systems may often be sufficiently fast that stream profiles within karst conduits do not have time to adjust their long profiles and erosion rates to accommodate changes in the rate of base level rise and fall.

4 A dissolving and leaky conveyor

The most basic concepts within the conveyor model remain intact within carbonate settings – rock is uplifted toward Earth's surface, it undergoes weathering, and the products of weathering are transported seaward. However, the details of the conceptual model need revision because of two fundamental ways in which carbonate settings diverge from the standard conveyor model. First, congruent weathering causes a large fraction of the total weathering flux to be exported from the system in a dissolved form. Second, the development of integrated subsurface drainage networks with high permeability and rapid, often turbulent, flow, allow solid weathering products to be transmitted to base level via subsurface conduits rather than along hillslopes and surface streams. Each of these two factors can be quantified using a dimensionless weathering flux fraction that varies between zero and one, with the first factor being quantified by

$$F_{dissolved} = \frac{W_{dissolved}}{W_{dissolved} + W_{solid}}, \quad (2)$$

where $W_{\text{dissolved}}$ is the dissolved weathering flux, W_{solid} is the solid weathering flux, and $F_{\text{dissolved}}$ is the fraction of dissolved flux, and where all fluxes have dimensions of M L^{-2} T^{-1}. The second factor is quantified by

$$F_{solid,sub} = \frac{W_{solid,sub}}{W_{solid,sub} + W_{solid,surf}}, \quad (3)$$

where $W_{\text{solid,sub}}$ is the solid weathering flux that transits through subsurface conduits, $W_{\text{solid,surf}}$ is the solid weathering flux that remains near the surface and is transmitted to base level via hillslopes and surface channels, and $F_{\text{solid,sub}}$ is the fraction of the solid weathering flux that transits through subsurface conduits. We consider two modified versions of the conveyor model, which we call the "dissolving conveyor" (where $F_{\text{dissolved}}$ is large) and the "leaky conveyor"

(where $F_{solid,sub}$ is large). Both modifications of the original conveyor model result in a weakening of the negative feedback mechanisms that drive weathering rates toward uplift rates and produce equilibrium landscapes. The dissolving conveyor describes settings where the dissolved fraction of the total seaward flux of weathering products is close to one, meaning that most weathered materials exit the system as solutes. In this case, the buildup of soil and regolith is insufficient to retard denudation. In cases where tectonic uplift is rapid, topography may become extremely steep, until mechanical weathering and erosion processes match uplift (Ott et al., 2019). In this case, the system would be driven away from the dissolving conveyor state as solid material export increases due to steepened terrain. In contrast, where uplift trate is low, the lack of negative feedback enables the development of karst planation surfaces (e.g. Krklec et al. 2022 ; Simms, 2004; Smart et al. 1986). In this case, surface denudation is not arrested until the land surface approaches base level and the water table.

The leaky conveyor describes settings where the fraction of solid weathering products transported through the karst conduit network is high, meaning that both solid and dissolved weathering materials transit through the subsurface to base level rather than down hillslopes and stream channels. This fraction should govern the ability of karst landscapes to develop, with high subsurface flux fractions producing landscapes dominated by dolines (Figure 10) and lacking integrated surface drainage networks. Again, this subsurface transport weakens feedback between uplift, weathering, and erosion, as base level changes may not communicate through the subsurface as they would in a surface stream network. In such cases, autogenic processes may drive patterns in topography and regolith thickness (e.g., Dong et al., 2018) rather than external forcing by tectonics.

While each of these modified models can be considered separately, there is likely a strong correlation between the two governing dimensionless fractions in real landscapes. Settings with a higher fraction of dissolved weathering fluxes will tend to have a higher percentage of weathering fluxes transiting through the conduit network. In these settings, karst conduit networks will be better developed than where solid weathering products dominate as a result of reduction in the total volume of insoluble weathering products. Importantly, both of these weathering flux fractions could be quantified via field studies. While there are some studies that quantify the relative importance of chemical and physical fluxes (e.g. Erlander et al., 2021; Ott et al., 2019), we are not aware of any studies that have quantified surface vs. subsurface fluxes. The controls on these both flux fractions are currently poorly constrained. While position on the carbonate-silicate spectrum is undoubtedly important, other factors, such as climate and tectonics, should also impact these flux fractions. Further work is also needed to elucidate the impacts that these weathering flux fractions, and their external controls, have on CZ architecture, dynamics, and resilience.

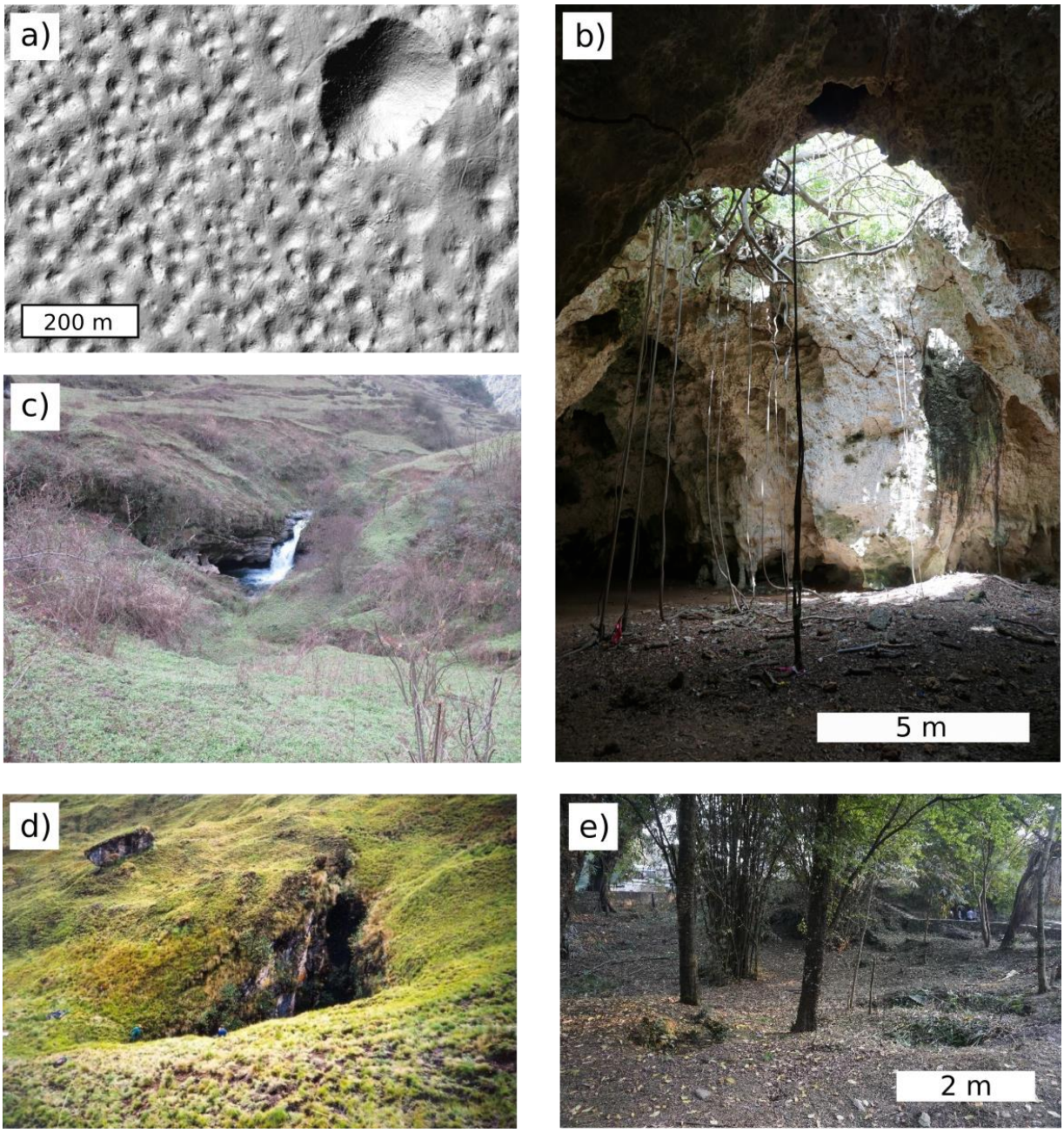

Figure 10. Dolines/sinkholes and shafts in karst terrains. a) A lidar hillshade of solution dolines, and a collapse doline, on Logaška Planota, Slovenia. b) Vegetation hangs into a collapse doline in a cave system on the island of Zanzibar. c) A stream channel within a blind valley sinks into a doline near the contact with carbonate rocks in Wulong County, China. d) A 60-meter-deep vertical shaft breaches a hillslope in the Andes of northern Peru (note cavers for scale). e) Small solutional dolines developed in a calcite-cemented conglomerate near Pokhara, Nepal.

5 Conclusions

Carbonates underlie a substantial portion of Earth's surface and represent an important fraction of Earth's CZ, providing crucial water resources and ecosystem services to more than a billion people. Our current state of knowledge suggests that the congruent weathering, high

solubility, and fast kinetics of carbonate dissolution, lead to altered rates and patterns of CZ evolution in carbonates compared to silicate settings. When landscapes develop in relatively pure carbonate rocks, karst systems typically form, producing large contrasts in subsurface permeability and long-range subsurface connectivity that enable rapid fluxes of water, solutes, sediment, and gases through the CZ along routes of preferential flow. Direct relationships between biological CO_2 production and carbonate weathering by carbonic acid mean that production of porosity in the subsurface may be tied to biological processes in carbonates, potentially enabling carbonate-specific feedback loops between CZ development and ecosystem form and function. Because of the rapid kinetics of calcite dissolution, shifts in system dynamics and structure due to changes in ecology, land use, or climate may also be rapid.

These differences show that conceptual models developed to understand CZ architecture and evolution within silicate-rich rocks, such as the conveyor model, may require rethinking in their application to carbonates. We present the initial ideas of a "dissolving conveyor" and a "leaky conveyor" as starting points to incorporate carbonate CZ processes. The ability of karst conduits to transport mobile regolith can lead to decoupling of hillslopes from stream channels, potentially weakening or eliminating feedback mechanisms that drive landscapes underlain by silicate-rich rocks toward equilibrium topography and regolith thickness. The fast reaction kinetics and elevated solubility of carbonate minerals lead to distinct differences in the relationships between tectonism and carbonate and silicate CZ development, including in the interactions between base level and the depths of weathering processes. Because of the deep circulation of meteoric water in karst settings, the lower boundary of the CZ needs to be expanded, and the definition of the CZ may need modification to include carbonate terrains.

A better understanding of carbonate CZ development may inspire broader conceptual frameworks that incorporate roles for preferential flow and heterogeneity, which are present to some extent in all CZ settings. The triple porosity system of matrix, fractures, and karst provides opportunities to study a spectrum of flow-through timescales and weathering rates and depths in one setting. Scaling questions are also amplified when there are large contrasts in permeability that vary with the scale considered. The controlling processes in the conveyor model for weathering might be better understood by measuring rates in a faster transport system, particularly under anthropogenic stresses, harking back to the concept of carbonate rocks as a bellwether. Constraining the transport of gases through the subsurface may enhance our understanding of the global carbon cycle and how it is affected by biological and geochemical processes.

Understanding how the CZ evolves along the carbonate-silicate spectrum requires a broader conceptual framework than we currently have. Many questions arise. What controls the distribution of CO_2 in the subsurface? How do advective processes influence this distribution? How do pCO_2, water availability, plant growth, and rock structure interact to determine patterns of porosity development? Under what conditions do acids other than carbonic acid drive porosity development? How are feedbacks between biological, hydrological, and geological processes reflected at the landscape scale? What factors control the partitioning of weathering fluxes between dissolved vs. solid and subsurface vs. surface? How does this partitioning impact the dynamics and structure of the CZ? There is also a need to integrate knowledge across sites rather than focusing on the idiosyncratic or distinctive nature of individual sites. In addition to pure carbonates and pure silicates, there is an entire spectrum of mixtures that lie between these

endmembers. What are the most important parameters along that spectrum that produce differences in CZ processes and architecture? Answers to these questions will require transdisciplinary study teams that are integrated into the CZ research community going forward.

Acknowledgments

This work was supported by the National Science Foundation grant CZ RCN: Research Coordination Network in Carbonate Critical Zones (1905259). PLS was also supported by CZ RCN: Expanding Knowledge of Earth's Critical Zone (1904527).

Open Research

No new data were presented in this review article.

References

Adams, C. S., & Swinnerton, A. C. (1937). Solubility of limestone. *Eos, Transactions American Geophysical Union*, *18*(2), 504-508.

Adams, P. N., Opdyke, N. D., & Jaeger, J. M. (2010). Isostatic uplift driven by karstification and sea-level oscillation: Modeling landscape evolution in north Florida. *Geology*, *38*(6), 531-534. https://doi.org/10.1130/G30592.1

Allred, K. (2004). Some carbonate erosion rates of southeast Alaska. *Journal of Cave and Karst Studies*, *66*(3), 89-97.

Álvarez Nazario, M. (1972). La herencia lingüística de Canarias en Puerto Rico. *San Juan: Instituto de Cultura Puertorriqueña,* 136-151.

Amundson, R., Richter, D. D., Humphreys, G. S., Jobbágy, E. G., & Gaillardet, J. (2007). Coupling between biota and earth materials in the critical zone. *Elements*, *3*(5), 327-332. https://doi.org/10.2113/gselements.3.5.327

1054 Anderson, R. S., Anderson, S. P., & Tucker, G. E. (2013). Rock damage and regolith transport
1055 by frost: An example of climate modulation of the geomorphology of the critical zone. *Earth*
1056 *Surface Processes and Landforms*, *38*(3), 299-316. https://doi.org/10.1002/esp.3330
1057 Anderson, S. P., Dietrich, W. E., & Brimhall Jr, G. H. (2002). Weathering profiles, mass-balance
1058 analysis, and rates of solute loss: Linkages between weathering and erosion in a small, steep
1059 catchment. *Geological Society of America Bulletin*, *114*(9), 1143-1158.
1060 https://doi.org/10.1130/0016-7606(2002)114<1143:WPMBAA>2.0.CO;2
1061 Andrews, J. A., & Schlesinger, W. H. (2001). Soil CO2 dynamics, acidification, and chemical
1062 weathering in a temperate forest with experimental CO2 enrichment. *Global biogeochemical*
1063 *cycles*, *15*(1), 149-162. https://doi.org/10.1029/2000GB001278
1064 Ashton, K. (1966). The analysis of flow data from karst drainage systems. *Transactions of the*
1065 *Cave Research Group of Great Britain*, 7(2), 161–204.
1066 Atkinson, T. C. (1977a). Diffuse flow and conduit flow in limestone terrain in the Mendip Hills,
1067 Somerset (Great Britain). *Journal of Hydrology*, *35*(1-2), 93–110. https://doi.org/10.1016/0022-
1068 1694(77)90079-8
1069 Atkinson, T. C. (1977b). Carbon dioxide in the atmosphere of the unsaturated zone: An
1070 important control of groundwater hardness in limestones. *Journal of Hydrology*, *35*(1-2), 111–
1071 123. https://doi.org/10.1016/0022-1694(77)90080-4
1072 Audra, P., Bini, A., Gabrovšek, F., Häuselmann, P., Hobléa, F., Jeannin, P.-Y., Kunaver, J.,
1073 Monbaron, M., Šušteršič, F., Tognini, P., Trimmel, H., Wildberger, A. (2007). Cave and Karst
1074 Evolution in the Alps and Their Relation to Paleoclimate and Paleotopography. *Acta*
1075 *Carsologica*, *36*(1), 53-67. https://doi.org/10.3986/ac.v36i1.208

1076 Back, W., Hanshaw, B.B., Herman, J.S., Van Driel, J.N. (1986). Differential dissolution of a
1077 Pleistocene reef in the ground-water mixing zone of coastal Yucatan, Mexico. *Geology, 14*(2),
1078 137–140.
1079 Baldini, J. U., Bertram, R. A., & Ridley, H. E. (2018). Ground air: A first approximation of the
1080 Earth's second largest reservoir of carbon dioxide gas. *Science of the Total Environment*, 616,
1081 1007-1013.
1082 Balestra, V., & Bellopede, R. (2022). Microplastic pollution in show cave sediments: First
1083 evidence and detection technique. *Environmental Pollution*, *292*, 118261.
1084 Bard, E., Antonioli, F., & Silenzi, S. (2002). Sea-level during the penultimate interglacial period
1085 based on a submerged stalagmite from Argentarola Cave (Italy). *Earth and Planetary Science*
1086 *Letters*, 196(3-4), 135-146.
1087 Beach, T., Luzzadder-Beach, S., Cook, D., Dunning, N., Kennett, D. J., Krause, S., ... & Valdez,
1088 F. (2015). Ancient Maya impacts on the Earth's surface: An Early Anthropocene analog?.
1089 *Quaternary Science Reviews*, *124*, 1-30.
1090 Beaulieu, E., Y. Goddéris, D. Labat, C. Roelandt, D. Calmels, and J. Gaillardet (2011),
1091 Modeling of water-rock interaction in the Mackenzie basin: Competition between
1092 sulfuric and carbonic acids, *Chemical Geology, 289*(1-2), 114-123.
1093 https://doi.org/10.1016/j.chemgeo.2011.07.020
1094 Beerling, D. J., Woodward, F. I., Lomas, M. R., Wills, M. A., Quick, W. P., & Valdes, P. J.
1095 (1998). The influence of Carboniferous palaeoatmospheres on plant function: an experimental
1096 and modelling assessment. *Philosophical Transactions of the Royal Society of London. Series B:*
1097 *Biological Sciences*, *353*(1365), 131-140. https://doi.org/10.1098/rstb.1998.0196

1098 Benavente, J., Vadillo, I., Carrasco, F., Soler, A., Liñán, C., Moral, F. (2010). Air Carbon
1099 Dioxide Contents in the Vadose Zone of a Mediterranean Karst. *Vadose Zone Journal, 9*(1), 126-
1100 136. https://doi.org/10.2136/vzj2009.0027
1101 Berner, R.A. (1992). Weathering, plants, and the long-term carbon cycle. *Geochimica et*
1102 *Cosmochimica Acta, 56*(8), 3225–3231. https://doi.org/10.1016/0016-7037(92)90300-8
1103 Berner, R.A. (1997). The Rise of Plants and Their Effect on Weathering and Atmospheric CO2.
1104 *Science, 276*(5312), 544–546. https://doi.org/10.1126/science.276.5312.544
1105 Billings, S. A., Hirmas, D., Sullivan, P. L., Lehmeier, C. A., Bagchi, S., Min, K. et al. (2018).
1106 Loss of deep roots limits biogenic agents of soil development that are only partially restored by
1107 decades of forest regeneration. *Elementa: Science of the Anthropocene, 6*(34).
1108 https://doi.org/10.1525/elementa.287
1109 Birk, S., Liedl, R., & Sauter, M. (2006). Karst Spring Responses Examined by Process-Based
1110 Modeling. *Ground Water, 44*(6), 832–836. https://doi.org/10.1111/j.1745-6584.2006.00175.x
1111 Bögli, A. (1964). Mischungskorrosion — Ein Beitrag zum Verkarstungsproblem. *Erdkunde, 18*,
1112 83–92.
1113 Brantley, S. L., Eissenstat, D. M., Marshall, J. A., Godsey, S. E., Balogh-Brunstad, Z., Karwan,
1114 D. L., et al. (2017). Reviews and syntheses: on the roles trees play in building and plumbing the
1115 critical zone. *Biogeosciences*, *14*(22), 5115-5142.
1116 Brantley, S.L., Holleran, M.E., Jin, L., & Bazilevskaya, E. (2013). Probing deep weathering in
1117 the Shale Hills Critical Zone Observatory, Pennsylvania (USA): the hypothesis of nested
1118 chemical reaction fronts in the subsurface. *Earth Surf. Process. Landforms, 38*(11), 1280–1298.
1119 https://doi.org/10.1002/esp.3415

Brantley, S.L., Lebedeva, M.I., Balashov, V.N., Singha, K., Sullivan, P.L., & Stinchcomb, G. (2017a). Toward a conceptual model relating chemical reaction fronts to water flow paths in hills. *Geomorphology, 277*, 100–117. https://doi.org/10.1016/j.geomorph.2016.09.027

Brantley, S.L., McDowell, W.H., Dietrich, W.E., White, T.S., Kumar, P., Anderson, S.P., Chorover, J., Lohse, K.A., Bales, R.C., Richter, D.D., Grant, G., & Gaillardet, J. (2017b). Designing a network of critical zone observatories to explore the living skin of the terrestrial Earth. *Earth Surface Dynamics, 5*(4), 841–860. https://doi.org/10.5194/esurf-5-841-2017

Breithaupt, C. I., Gulley, J. D., Bunge, E. M., Moore, P. J., Kerans, C., Fernandez-Ibanez, F., & Fullmer, S. M. (2021). A transient, perched aquifer model for banana hole formation: Evidence from San Salvador Island, Bahamas. *Earth Surface Processes and Landforms, 47*(2), 618-638. https://doi.org/10.1002/esp.5276

Brookfield, A.E., Macpherson, G.L., & Covington, M.D. (2017). Effects of Changing Meteoric Precipitation Patterns on Groundwater Temperature in Karst Environments. *Groundwater, 55*2(2), 227–236. https://doi.org/10.1111/gwat.12456

Brown, A.L., Martin, J.B., Screaton, E.J., Ezell, J.E., Spellman, P., & Gulley, J. (2014). Bank storage in karst aquifers: The impact of temporary intrusion of river water on carbonate dissolution and trace metal mobility. *Chemical Geology, 385*, 56–69. https://doi.org/10.1016/j.chemgeo.2014.06.015

Brown, A.L., Martin, J.B., Kamenov, G.D., Ezell, J.E., Screaton, E.J., Gulley, J., & Spellman, P. (2019). Trace metal cycling in karst aquifers subject to periodic river water intrusion. *Chemical Geology, 527*, 118773. https://doi.org/10.1016/j.chemgeo.2018.05.020

1141 Brucker, R.W., Hess, J.W., & White, W.B., 1972. Role of Vertical Shafts in the Movement of
1142 Ground Water in Carbonate Aquifers. *Groundwater, 10*(6), 5–13. https://doi.org/10.1111/j.1745-
1143 6584.1972.tb02943.x
1144 Brumm, A., Oktaviana, A. A., Burhan, B., Hakim, B., Lebe, R., Zhao, J. X., ... & Aubert, M.
1145 (2021). Oldest cave art found in Sulawesi. *Science Advances*, *7*(3), eabd4648.
1146 Buhmann, D., & Dreybrodt, W. (1985a). The kinetics of calcite dissolution and precipitation in
1147 geologically relevant situations of karst areas: 1. Open system. *Chemical geology*, 48(1-4), 189-
1148 211.
1149 Buhmann, D., & Dreybrodt, W. (1985b). The kinetics of calcite dissolution and precipitation in
1150 geologically relevant situations of karst areas: 2. Closed system. *Chemical Geology*, 53(1-2),
1151 109-124.
1152 Chen, X., Zhang, Z., Soulsby, C., Cheng, Q., Binley, A., Jiang, R., & Tao, M. (2018).
1153 Characterizing the heterogeneity of karst critical zone and its hydrological function: an integrated
1154 approach. *Hydrological Processes*, 32(19), 2932-2946.
1155 Choquette, P. W., & L. E. Pray (1970), Geologic nomenclature and classification of porosity in
1156 sedimentary carbonates, *American Association of Petroleum Geologists Bulletin*, *54*(2), 207-250.
1157 https://doi.org/10.1306/5D25C98B-16C1-11D7-8645000102C1865D
1158 Cohen, M. J., Watts, D. L., Heffernan, J. B., & Osborne, T. Z. (2011). Reciprocal biotic control
1159 on hydrology, nutrient gradients, and landform in the greater everglades. *Critical Reviews in*
1160 *Environmental Science and Technology*, *41*(S1), 395-429.
1161 https://doi.org/10.1080/10643389.2010.531224

1162 Condon, L. E., Markovich, K. H., Kelleher, C. A., McDonnell, J. J., Ferguson, G., & McIntosh,
1163 J. C. (2020). Where is the bottom of a watershed?. *Water Resources Research*, *56*(3),
1164 e2019WR026010. https://doi.org/10.1029/2019WR026010.
1165 Cooper, M.P., & Covington, M.D. (2020). Modeling cave cross-section evolution including
1166 sediment transport and paragenesis. *Earth Surface Processes and Landforms*, *45*(11), 2588–
1167 2602. https://doi.org/10.1002/esp.4915
1168 Covington, M. D. (2014). Calcite dissolution under turbulent flow conditions: a remaining
1169 conundrum. *Acta Carsologica*, *43*(1).
1170 Covington, M.D. (2016). The importance of advection for CO2 dynamics in the karst critical
1171 zone: An approach from dimensional analysis, in: *Geological Society of America Special Papers*
1172 *516: Caves and Karst Across Time*, Geological Society of America, pp. 113–127.
1173 https://doi.org/10.1130/2015.2516(09)
1174 Covington, M. D., Knierim, K. J., Young, H. A., Rodriguez, J., & Gnoza, H. G. (2021). The
1175 impact of ventilation patterns on calcite dissolution rates within karst conduits. *Journal of*
1176 *Hydrology*, *593*, 125824. https://doi.org/10.1016/j.jhydrol.2020.125824
1177 Covington, M. D., Luhmann, A. J., Wicks, C. M., & Saar, M. O. (2012). Process length scales
1178 and longitudinal damping in karst conduits. *Journal of Geophysical Research: Earth Surface*,
1179 *117*(F1). https://doi.org/10.1029/2011JF002212
1180 Covington, M. D., & Perne, M. (2015). Consider a cylindrical cave: A physicist's view of cave
1181 and karst science. *Acta Carsologica*, *44*(3).
1182 Covington, M.D., Prelovšek, M., & Gabrovšek, F. (2013). Influence of CO2 dynamics on the
1183 longitudinal variation of incision rates in soluble bedrock channels: feedback mechanisms,
1184 *Geomorphology*, *186*, 85-95, https://doi:10.1016/j.geomorph.2012.12.025.

1185 Covington, M.D., Vaughn, K.A. (2019). Carbon dioxide and dissolution rate dynamics within a
1186 karst underflow-overflow system, Savoy Experimental Watershed, Arkansas, USA. *Chemical*
1187 *Geology, 527*, 118689. https://doi.org/10.1016/j.chemgeo.2018.03.009
1188 Culver, D.C., Pipan, T., 2013. Subterranean Ecosystems, in: Levin, S.A. (Ed), *Encyclopedia of*
1189 *Biodiversity*. Academic Press, pp. 49–62. https://doi.org/10.1016/B978-0-12-384719-5.00224-0
1190 Cvijić, J. (1924). Types morphologiques des terrains calcaires. *Bulletin of the Serbian*
1191 *geographical society*, *10*(1), 1-7.
1192 D'Angeli, I. M., Parise, M., Vattano, M., Madonia, G., Galdenzi, S., & De Waele, J. (2019).
1193 Sulfuric acid caves of Italy: A review. *Geomorphology*, *333*, 105-122.
1194 https://doi.org/10.1016/j.geomorph.2019.02.025.
1195 Dammeyer, H. C., Schwinning, S., Schwartz, B. F., & Moore, G. W. (2016). Effects of juniper
1196 removal and rainfall variation on tree transpiration in a semi-arid karst: Evidence of complex
1197 water storage dynamics. *Hydrological Processes*, *30*, 4568–4581.
1198 Davis, D.G., 1980. Cave development in the Guadalupe Mountains: a critical review of recent
1199 hypotheses. *NSS Bulletin, 42*, 42–48.
1200 Davis, D. M., & Engelder, T. (1985). The role of salt in fold-and-thrust belts. *Tectonophysics*,
1201 *119*(1-4), 67-88.
1202 Day, C. C., von Strandmann, P. A. P., & Mason, A. J. (2021). Lithium isotopes and partition
1203 coefficients in inorganic carbonates: Proxy calibration for weathering reconstruction.
1204 *Geochimica et Cosmochimica Acta*, *305*, 243-262.
1205 Deng, Y., Jiang, Z., & Qin, X. (2012). Water source partitioning among trees growing on
1206 carbonate rock in a subtropical region of Guangxi, China. *Environmental Earth Sciences, 66*,
1207 635–640.

1208 Deuerling, K. M., Martin, J. B., Martin, E. E., Abermann, J., Myreng, S. M., Petersen, D., &
1209 Rennermalm, Å. K. (2019). Chemical weathering across the western foreland of the Greenland
1210 Ice Sheet. *Geochimica et Cosmochimica Acta*, *245*, 426-440.
1211 Dominguez-Cristobal, C. (1989). *La Toponomia del Ciales decimonónico (Vol. 1)*. Instituto
1212 Internacional de Dasonomía Tropical, San Juan.
1213 Dominguez-Cristobal, C. (1992). *La Toponomia del Ciales decimonónico (Vol. 2)*. Instituto
1214 Internacional de Dasonomía Tropical, San Juan.
1215 Cristóbal, C. M. D. (2007). Leyendas indigenas de la zona del carso norteño de Puerto Rico: el
1216 caliche de Ciales. *Acta Cientifica*, *21*(1-3), 81-83.
1217 Dong, X., Cohen, M. J., Martin, J. B., McLaughlin, D. L., Murray, A. B., Ward, N. D., et al.
1218 (2019a). Ecohydrologic processes and soil thickness feedbacks control limestone-weathering
1219 rates in a karst landscape. *Chemical Geology*, *527*, 118774.
1220 https://doi.org/10.1016/j.chemgeo.2018.05.021
1221 Dong, X., Murray, A.B., & Heffernan, J.B. (2019b). Ecohydrologic feedbacks controlling sizes
1222 of cypress wetlands in a patterned karst landscape. *Earth Surface Processes and Landforms, 44*,
1223 1178–1191. https://doi.org/10.1002/esp.4564
1224 Drake, J. J. (1980). The effect of soil activity on the chemistry of carbonate groundwaters. *Water*
1225 *Resources Research*, *16*(2), 381-386. https://doi.org/10.1029/WR016i002p00381
1226 Drever, J.I. (1994). The effect of land plants on weathering rates of silicate minerals. *Geochimica*
1227 *et Cosmochimica Acta, 58*, 2325–2332. https://doi.org/10.1016/0016-7037(94)90013-2
1228 Dreybrodt, W. (1990). The Role of Dissolution Kinetics in the Development of Karst Aquifers in
1229 Limestone: A Model Simulation of Karst Evolution. *The Journal of Geology, 98*, 639–655.

1230 Dreybrodt, W. (1996). Principles of Early Development of Karst Conduits Under Natural and
1231 Man-Made Conditions Revealed by Mathematical Analysis of Numerical Models. *Water Resour.*
1232 *Res.*, *32*, 2923–2935. https://doi.org/10.1029/96WR01332
1233 Druhan, J. L., Lawrence, C. R., Covey, A. K., Giannetta, M. G., & Oster, J. L. (2021). A reactive
1234 transport approach to modeling cave seepage water chemistry I: Carbon isotope transformations.
1235 *Geochimica et Cosmochimica Acta*, 311, 374-400.
1236 C. Dubois, Y. Quinif, J.-M. Baele, L. Barriquand, A. Bini, L. Bruxelles, G. Dandurand, C.
1237 Havron, O. Kaufmann, B., Lans, R. Maire, J. Martin, J. Rodet, M.D., et al. (2014). The process
1238 of ghost-rock karstification and its role in the formation of cave systems, *Earth Sci. Rev.*, 131,
1239 166-148.
1240 Engel, A. S., L. A. Stern, & P. C. Bennett (2004), Microbial contributions to cave formation:
1241 New insights into sulfuric acid speleogenesis, *Geology*, *32*(5), 369-372.
1242 Egemeier, S.J. (1987). A theory for the origin of Carlsbad Caverns. *NSS Bulletin. 49*, 73–76.
1243 Egemeier, S. J. (1988), Cavern development by thermal water, *NSS Bulletin*, *43*, 31-51.
1244 Ellsworth, P. Z., & Sternberg, L. S. L. (2015). Seasonal water use by deciduous and evergreen
1245 woody species in a scrub community is based on water availability and root distribution.
1246 *Ecohydrology*, *8*, 538–551.
1247 Erlanger, E. D., Rugenstein, J. K. C., Bufe, A., Picotti, V., & Willett, S. D. (2021). Controls on
1248 Physical and Chemical Denudation in a Mixed Carbonate-Siliciclastic Orogen. *Journal of*
1249 *Geophysical Research: Earth Surface*, *126*(8), e2021JF006064.
1250 Estrada-Medina, H., Graham, R. C., Allen, M. F., Jiménez-Osornio, J. J., & Robles-Casolco, S.
1251 (2013). The importance of limestone bedrock and dissolution karst features on tree root
1252 distribution in northern Yucatán, México. *Plant and soil*, *362*(1), 37-50.

1253 Ewers, O.R. (1982). *Cavern development in the dimensions of length and breadth* (Doctoral
1254 dissertation). Hamilton, Canada: McMaster University.
1255 Faimon, J., Lang, M., Geršl, M., Sracek, O., & Bábek, O. (2020). The "breathing spots" in karst
1256 areas—the sites of advective exchange of gases between soils and adjacent underground cavities.
1257 *Theoretical and Applied Climatology*, *142*(1), 85-101. https://doi.org/10.1007/s00704-020-
1258 03280-7
1259 Fairchild, I. J., Smith, C. L., Baker, A., Fuller, L., Spötl, C., Mattey, D., & McDermott, F.
1260 (2006). Modification and preservation of environmental signals in speleothems. *Earth-Science*
1261 *Reviews*, *75*(1-4), 105-153. https://doi.org/10.1016/j.earscirev.2005.08.003
1262 Farrant, A.R., & Smart, P.L. (2011). Role of sediment in speleogenesis; sedimentation and
1263 paragenesis. *Geomorphology, 134*, 79–93. https://doi.org/10.1016/j.geomorph.2011.06.006
1264 Filipponi, M., Jeannin, P.-Y., & Tacher, L. (2009). Evidence of inception horizons in karst
1265 conduit networks. *Geomorphology, 106*, 86–99. https://doi.org/10.1016/j.geomorph.2008.09.010
1266 Fischedick, M., Roy, J., Acquaye, A., Allwood, J., Ceron, J. P., Geng, Y., et al. (2014). Industry
1267 In: *Climate Change 2014: Mitigation of Climate Change. Contribution of Working Group III to*
1268 *the Fifth Assessment Report of the Intergovernmental Panel on Climate Change.* Technical
1269 Report. Cambridge University Press, Cambridge, United Kingdom.
1270 Flint, M. K., Martin, J. B., Summerall, T. I., Barry-Sosa, A., & Christner, B. C. (2021). Nitrous
1271 oxide processing in carbonate karst aquifers. *Journal of hydrology*, *594*, 125936.
1272 Florea, L.J., & Vacher, H.L. (2006). Springflow Hydrographs: Eogenetic vs. Telogenetic Karst.
1273 *Ground Water, 44*, 352–361. https://doi.org/10.1111/j.1745-6584.2005.00158.x

1274 Florea, L.J., Vacher, H.L., Donahue, B., & Naar, D. (2007). Quaternary cave levels in peninsular
1275 Florida. *Quaternary Science Reviews*, *26*, 1344–1361.
1276 https://doi.org/10.1016/j.quascirev.2007.02.011
1277 Fohlmeister, J., Scholz, D., Kromer, B., & Mangini, A. (2011). Modelling carbon isotopes of
1278 carbonates in cave drip water. *Geochimica et Cosmochimica Acta*, 75(18), 5219-5228.
1279 Fohlmeister, J., Voarintsoa, N.R.G., Lechleitner, F.A., Boyd, M., Brandtstätter, S., Jacobson,
1280 M.J., & Oster, J.L. (2020). Main controls on the stable carbon isotope composition of
1281 speleothems. *Geochimica et Cosmochimica Acta, 279*, 67–87.
1282 https://doi.org/10.1016/j.gca.2020.03.042
1283 Ford, D. C. (1971). Alpine Karst in the Mt. Castleguard-Columbia icefield area, Canadian Rocky
1284 Mountains. *Arctic and Alpine Research*, *3*(3), 239-252.
1285 Ford, D. C., Lauritzen, S. E., & Ewers, R. O. (2000). Modeling of initiation and propagation of
1286 single conduits and networks. *Speleogenesis: Evolution of Karst Aquifers. Huntsville, Ala., National Speleological Society*, 175-183.
1287
1288 Ford, D., & Williams, P.D. (2007). *Karst hydrogeology and geomorphology*. John Wiley &
1289 Sons.
1290 Frumkin, A., 2013. Salt karst. In: Shroder, J. (Editor in Chief), Frumkin, A. (Ed.), *Treatise on*
1291 *Geomorphology, Karst Geomorphology*. Academic Press, San Diego, CA, 407-424.
1292 Fu, T., Chen, H., Fu, Z., & Wang, K. (2016). Surface soil water content and its controlling
1293 factors in a small karst catchment. *Environmental Earth Sciences, 75*, 1406.
1294 Gabrovšek, F. (2009). On concepts and methods for the estimation of dissolutional denudation
1295 rates in karst areas. *Geomorphology, 106*, 9–14. https://doi.org/10.1016/j.geomorph.2008.09.008

1296 Gabrovšek, F., & Dreybrodt, W. (2001). A model of the early evolution of karst aquifers in
1297 limestone in the dimensions of length and depth. *Journal of Hydrology, 240*, 206–224.
1298 https://doi.org/10.1016/S0022-1694(00)00323-1
1299 Gabrovšek, F., Häuselmann, P., & Audra, P. (2014). 'Looping caves' versus 'water table caves':
1300 The role of base-level changes and recharge variations in cave development. *Geomorphology,*
1301 *204*, 683–691. https://doi.org/10.1016/j.geomorph.2013.09.016
1302 Gaillardet, J., Braud, I., Hankard, F., Anquetin, S., Bour, O., Dorfliger, N., ... & Zitouna, R.
1303 (2018). OZCAR: The French network of critical zone observatories. *Vadose Zone Journal*, 17(1),
1304 1-24.
1305 Gaillardet, J., Calmels, D., Romero-Mujalli, G., Zakharova, E., & Hartmann, J. (2019). Global
1306 climate control on carbonate weathering intensity. *Chemical Geology*, *527*, 118762.
1307 https://doi.org/10.1016/j.chemgeo.2018.05.009
1308 Galloway, J. N. (1998). The global nitrogen cycle: changes and consequences. *Environmental*
1309 *pollution*, *102*(1), 15-24.
1310 Galloway, J. N., Townsend, A. R., Erisman, J. W., Bekunda, M., Cai, Z., Freney, J. R., et al.
1311 (2008). Transformation of the nitrogen cycle: recent trends, questions, and potential solutions.
1312 *Science*, *320*(5878), 889-892.
1313 Gandois, L., A.-S. Perrin, & A. Probst (2011). Impact of nitrogenous fertiliser-induced proton
1314 release on cultivated soils with contrasting carbonate contents: a column experiment.
1315 *Geochimica et cosmochimica acta, 75*(5): 1185-1198.
1316 Garcia, A. A., Semken, S., & Brandt, E. (2020). The Construction of Cultural Consensus Models
1317 to Characterize Ethnogeological Knowledge. *Geoheritage*, *12*(3), 59.
1318 https://doi.org/10.1007/s12371-020-00480-5

1319 Geekiyanage, N., Goodale, U. M., Cao, K., & Kitajima, K. (2019). Plant ecology of tropical and
1320 subtropical karst ecosystems. *Biotropica*, *51*(5), 626-640.
1321 Goldscheider, N., Chen, Z., Auler, A. S., Bakalowicz, M., Broda, S., Drew, D., et al. (2020).
1322 Global distribution of carbonate rocks and karst water resources. *Hydrogeology Journal*, *28*(5),
1323 1661-1677. https://doi.org/10.1007/s10040-020-02139-5
1324 Gombert, P. (2002). Role of karstic dissolution in global carbon cycle. *Global and Planetary*
1325 *Change*, *33*, 177–184. https://doi.org/10.1016/S0921-8181(02)00069-3
1326 Gonzalez, B. C., Iliffe, T. M., Macalady, J. L., Schaperdoth, I., & Kakuk, B. (2011). Microbial
1327 hotspots in anchialine blue holes: initial discoveries from the Bahamas. *Hydrobiologia*, *677*(1),
1328 149-156.
1329 Granger, D.E., Fabel, D., & Palmer, A.N. (2001). Pliocene-Pleistocene incision of the Green
1330 River, Kentucky, determined from radioactive decay of cosmogenic 26Al and 10Be in Mammoth
1331 Cave sediments. *Geological Society of America Bulletin, 113*, 825–836.
1332 Green, S.M., Dungait, J.A.J., Tu, C., Buss, H.L., Sanderson, N., Hawkes, S.J., et al. (2019). Soil
1333 functions and ecosystem services research in the Chinese karst Critical Zone. *Chemical Geology*,
1334 *527*, 119107. https://doi.org/10.1016/j.chemgeo.2019.03.018
1335 Groves, C., & Hendrikson, M. (2011). From sink to resurgence: the buffering capacity of a cave
1336 system in the Tongass National Forest, USA. *Acta Carsologica, 391*.
1337 Groves, C.G., & Howard, A.D. (1994). Minimum hydrochemical conditions allowing limestone
1338 cave development. *Water Resour. Res., 30*, 607–615. https://doi.org/10.1029/93WR02945
1339 Groves, C., & Meiman, J. (2005). Weathering, geomorphic work, and karst landscape evolution
1340 in the Cave City groundwater basin, Mammoth Cave, Kentucky. *Geomorphology*, *67*, 115–126.
1341 https://doi.org/10.1016/j.geomorph.2004.07.008

1342 Gulley, J.D., Martin, J.B., & Brown, A. (2016). Organic carbon inputs, common ions and
1343 degassing: rethinking mixing dissolution in coastal eogenetic carbonate aquifers: Rethinking
1344 Mixing Dissolution in Coastal Eogenetic Carbonate Aquifers. *Earth Surf. Process. Landforms*,
1345 *41*, 2098–2110. https://doi.org/10.1002/esp.3975
1346 Gulley, J.D., Martin, J.B., Moore, P.J., Brown, A., Spellman, P.D., & Ezell, J. (2015).
1347 Heterogeneous distributions of CO2 may be more important for dissolution and karstification in
1348 coastal eogenetic limestone than mixing dissolution. *Earth Surf. Process. Landforms, 40*, 1057–
1349 1071. https://doi.org/10.1002/esp.3705
1350 Gulley, J.D., Martin, J.B., Moore, P.J., & Murphy, J. (2013). Formation of phreatic caves in an
1351 eogenetic karst aquifer by CO2 enrichment at lower water tables and subsequent flooding by sea
1352 level rise. *Earth Surf. Process. Landforms, 38*, 1210–1224. https://doi.org/10.1002/esp.3358
1353 Gulley, J., Martin, J., & Moore, P. (2014). Vadose CO2 gas drives dissolution at water tables in
1354 eogenetic karst aquifers more than mixing dissolution. *Earth Surf. Process. Landforms, 39*,
1355 1833–1846. https://doi.org/10.1002/esp.3571
1356 Gulley, J., Martin, J.B., Screaton, E.J., & Moore, P.J. (2011). River reversals into karst springs:
1357 A model for cave enlargement in eogenetic karst aquifers. *Geological Society of America*
1358 *Bulletin, 123*, 457–467. https://doi.org/10.1130/B30254.1
1359 Gulley, J., Martin, J., Spellman, P., Moore, P., & Screaton, E. (2013). Dissolution in a variably
1360 confined carbonate platform: effects of allogenic runoff, hydraulic damming of groundwater
1361 inputs, and surface-groundwater exchange at the basin scale. *Earth Surf. Process. Landforms*, *38*,
1362 1700–1713. https://doi.org/10.1002/esp.3411
1363 Gunn, J. (1981). Limestone solution rates and processes in the Waitomo district, New Zealand.
1364 *Earth Surface Processes and Landforms*, *6*(5), 427-445.

Gutiérrez, F., Parise, M., De Waele, J., & Jourde, H. (2014). A review on natural and human-induced geohazards and impacts in karst. *Earth-Science Reviews*, *138*, 61-88.

Haas, S., De Beer, D., Klatt, J. M., Fink, A., Rench, R. M., Hamilton, T. L., et al. (2018). Low-light anoxygenic photosynthesis and Fe-S-biogeochemistry in a microbial mat. *Frontiers in Microbiology*, *9*, 858.

Halihan, T., Sharp, J. M., & Mace, R. E. (2000). Flow in the San Antonio segment of the Edwards aquifer: matrix, fractures, or conduits?. In Sasowsky, I. D., & Wicks, C. M. (Eds), *Groundwater flow and contaminant transport in carbonate aquifers.* CRC Press. (pp. 129-146).

Hanna, R. B., & Rajaram, H. (1998). Influence of aperture variability on dissolutional growth of fissures in karst formations. *Water Resources Research*, *34*(11), 2843-2853. https://doi.org/10.1029/98WR01528

Hartmann, A., Goldscheider, N., Wagener, T., Lange, J., & Weiler, M. (2014). Karst water resources in a changing world: Review of hydrological modeling approaches. *Reviews of Geophysics*, *52*(3), 218-242.

Hartmann, A., Gleeson, T., Wada, Y., & Wagener, T. (2017). Enhanced groundwater recharge rates and altered recharge sensitivity to climate variability through subsurface heterogeneity. *Proceedings of the National Academy of Sciences*, *114*(11), 2842-2847.

Hartmann, A., Jasechko, S., Gleeson, T., Wada, Y., Andreo, B., Barberá, J. A., ... & Wagener, T. (2021). Risk of groundwater contamination widely underestimated because of fast flow into aquifers. *Proceedings of the National Academy of Sciences*, *118*(20), e2024492118.

Hartmann, J., & Moosdorf, N. (2012). The new global lithological map database GLiM: A representation of rock properties at the Earth surface. *Geochemistry, Geophysics, Geosystems*, *13*. https://doi.org/10.1029/2012GC004370

1388 Häuselmann, P., & Tognini, P. (2005). Kaltbach cave (Siebenhengste, Switzerland): Phantom of
1389 the sandstone? *Acta carsologica, 34*.
1390 Heimsath, A.M., Chadwick, O.A., Roering, J.J., & Levick, S.R. (2020). Quantifying erosional
1391 equilibrium across a slowly eroding, soil mantled landscape. *Earth Surface Processes and*
1392 *Landforms, 45*, 499–510. https://doi.org/10.1002/esp.4725
1393 Heimsath, A.M., Dietrich, W.E., Nishiizumi, K., & Finkel, R.C. (1997). The soil production
1394 function and landscape equilibrium. *Nature, 388*, 358–361. https://doi.org/10.1038/41056
1395 Hendy, C. H. (1971). The isotopic geochemistry of speleothems—I. The calculation of the
1396 effects of different modes of formation on the isotopic composition of speleothems and their
1397 applicability as palaeoclimatic indicators. *Geochimica et cosmochimica Acta*, 35(8), 801-824.
1398 Henry, P. J. (1978). *Mechanique lineaire de la rupture applique a l'etude de la fissuration et de*
1399 *la fracture de roches calcaires*, (Doctoral dissertation). Lille, France: Lille University of Science
1400 and Technology.
1401 Herman, E.K., Toran, L., & White, W.B. (2012). Clastic sediment transport and storage in
1402 fluviokarst aquifers: an essential component of karst hydrogeology. *Carbonates Evaporites, 27*,
1403 211–241. https://doi.org/10.1007/s13146-012-0112-7
1404 Hill, C.A. (1990). Sulfuric Acid Speleogenesis of Carlsbad Cavern and Its Relationship to
1405 Hydrocarbons, Delaware Basin, New Mexico and Texas. *AAPG Bulletin, 74*, 1685–1694.
1406 https://doi.org/10.1306/0C9B2565-1710-11D7-8645000102C1865D
1407 Hilley, G.E., Chamberlain, C.P., Moon, S., Porder, S., & Willett, S.D. (2010). Competition
1408 between erosion and reaction kinetics in controlling silicate-weathering rates. *Earth and*
1409 *Planetary Science Letters, 293*, 191–199. https://doi.org/10.1016/j.epsl.2010.01.008

1410 Houillon, N., Lastennet, R., Denis, A., Malaurent, P., Minvielle, S., & Peyraube, N. (2017).
1411 Assessing cave internal aerology in understanding carbon dioxide (CO2) dynamics: implications
1412 on calcite mass variation on the wall of Lascaux Cave (France). *Environ Earth Sci*, *76*, 170.
1413 https://doi.org/10.1007/s12665-017-6498-8
1414 Hu, M., & Hueckel, T. (2019). Modeling of subcritical cracking in acidized carbonate rocks via
1415 coupled chemo-elasticity. *Geomechanics for Energy and the Environment*, *19*, 100114.
1416 Huang, Y., Zhao, P., Zhang, Z., Li, X., He, C., & Zhang, R. (2009). Transpiration of
1417 Cyclobalanopsis glauca (syn. Quercus glauca) stand measured by sap-flow method in a karst
1418 rocky terrain during dry season. *Ecological Research*, *24*, 791–801.
1419 Irwin, J. G., & Williams, M. L. (1988). Acid rain: chemistry and transport. *Environmental*
1420 *Pollution*, *50*(1-2), 29-59.
1421 Jackson, R.B., Canadell, J., Ehleringer, J.R., Mooney, H.A., Sala, O.E., & Schulze, E.D. (1996).
1422 A global analysis of root distributions for terrestrial biomes. *Oecologia*, *108*, 389–411.
1423 https://doi.org/10.1007/BF00333714
1424 Jagnow, D.H., Hill, C.A., Davis, D.G., DuChene, H.R., Cunningham, K.I., Northup, D.E. et al.
1425 (2000). History of the sulfuric acid theory of speleogenesis in the Guadalupe Mountains, New
1426 Mexico. *Journal of Cave and Karst Studies*, *62*, 54–59.
1427 Jiang, Z., Lian, Y., & Qin, X. (2014). Rocky desertification in Southwest China: impacts, causes,
1428 and restoration. *Earth-Science Reviews*, *132*, 1-12.
1429 https://doi.org/10.1016/j.earscirev.2014.01.005.
1430 Jobbágy, E.G., & Jackson, R.B. (2000). The Vertical Distribution of Soil Organic Carbon and Its
1431 Relation to Climate and Vegetation. *Ecological Applications*, *10*, 423–436.
1432 https://doi.org/10.1890/1051-0761(2000)010[0423:TVDOSO]2.0.CO;2

1433 Jones, D. S., Polerecky, L., Galdenzi, S., Dempsey, B. A. & Macalady, J. L. (2015). Fate of
1434 sulfide in the Frasassi cave system and implications for sulfuric acid speleogenesis. *Chemical*
1435 *Geology, 410*, 21–27.
1436 Jourde, H., Massei, N., Mazzilli, N., Binet, S., Batiot-Guilhe, C., Labat, D., ... & Wang, X.
1437 (2018). SNO KARST: A French network of observatories for the multidisciplinary study of
1438 critical zone processes in karst watersheds and aquifers. *Vadose Zone Journal*, 17(1), 1-18.
1439 Khadka, M.B., Martin, J.B., & Jin, J. (2014). Transport of dissolved carbon and CO2 degassing
1440 from a river system in a mixed silicate and carbonate catchment. *Journal of Hydrology*, *513*,
1441 391–402.
1442 Kim, H., Stinchcomb, G., & Brantley, S.L. (2017). Feedbacks among O2 and CO2 in deep soil
1443 gas, oxidation of ferrous minerals, and fractures: A hypothesis for steady-state regolith thickness.
1444 *Earth and Planetary Science Letters*, *460*, 29–40. https://doi.org/10.1016/j.epsl.2016.12.003
1445 Király, L. (1975). Rapport sur l'état actuel des connaissances dans le domaine des caractères
1446 physiques des roches karstiques. *Hydrogeology of karstic terrains (Hydrogéologie des terrains*
1447 *karstiques) International Union of geological sciences, 3*, 53–67.
1448 Klappa, C. F. (1980). Brecciation textures and tepee structures in Quaternary calcrete (caliche)
1449 profiles from eastern Spain: the plant factor in their formation. *Geological Journal*, *15*(2), 81-89.
1450 Klimchouk, A. (2004). Towards defining, delimiting and classifying epikarst: Its origin,
1451 processes and variants of geomorphic evolution. *Speleogenesis and Evolution of Karst Aquifers*,
1452 *2*, 1–13.
1453 Klimchouk, A. B. (2007). Hypogene speleogenesis: Hydrogeological and Morphogenetic
1454 Perspective. NCKRI-Special Paper 1.
1455 Klimchouk, A. (2019). Krubera (Voronja) Cave, in: Encyclopedia of Caves. Elsevier, pp. 627–
1456 634.

1457 Klimchouk, A., Forti, P., & Cooper, A. (1996). Gypsum karst of the World: a brief overview.
1458 *International Journal of Speleology, 25*, 3-4, 159-181.
1459 Kogovšek, J., & Petrič, M. (2012). Characterization of the vadose flow and its influence on the
1460 functioning of karst springs: Case study of the karst system near Postojna, Slovenia. *Acta*
1461 *carsologica, 41*.
1462 Kowalczk, A.J., & Froelich, P.N. (2010). Cave air ventilation and CO2 outgassing by radon-222
1463 modeling: How fast do caves breathe? *Earth and Planetary Science Letters, 289*, 209–219.
1464 https://doi.org/10.1016/j.epsl.2009.11.010
1465 Krklec, K., Braucher, R., Perica, D., & Domínguez-Villar, D. (2022). Long-term denudation rate
1466 of karstic North Dalmatian Plain (Croatia) calculated from 36Cl cosmogenic nuclides.
1467 *Geomorphology, 413*, 108358.
1468 Kůrková, I., Bruthans, J., Balák, F., Slavík, M., Schweigstillová, J., Bruthansová, J., et al. (2019).
1469 Factors controlling evolution of karst conduits in sandy limestone and calcareous sandstone
1470 (Turnov area, Czech Republic). *Journal of Hydrology, 574*, 1062–1073.
1471 https://doi.org/10.1016/j.jhydrol.2019.05.013
1472 Lang, M., Faimon, J., Godissart, J., & Ek, C. (2017). Carbon dioxide seasonality in dynamically
1473 ventilated caves: the role of advective fluxes. *Theor Appl Climatol, 129*, 1355–1372.
1474 https://doi.org/10.1007/s00704-016-1858-y
1475 Larson, E.B., & Mylroie, J.E. (2018). Diffuse Versus Conduit Flow in Coastal Karst Aquifers:
1476 The Consequences of Island Area and Perimeter Relationships. *Geosciences, 8*, 268.
1477 https://doi.org/10.3390/geosciences8070268

1478 Lauritzen, S. E. (1990). Autogenic and allogenic denudation in carbonate karst by the multiple
1479 basin method: an example from Svartisen, north Norway. *Earth Surface Processes and*
1480 *Landforms*, *15*(2), 157-167.
1481 Lebedeva, M.I., Fletcher, R.C., Brantley, S.L. (2010). A mathematical model for steady-state
1482 regolith production at constant erosion rate. *Earth Surf. Process. Landforms, 35*, 508–524.
1483 https://doi.org/10.1002/esp.1954
1484 Lechleitner, F. A., Day, C. C., Kost, O., Wilhelm, M., Haghipour, N., Henderson, G. M., & Stoll,
1485 H. M. (2021). Stalagmite carbon isotopes suggest deglacial increase in soil respiration in western
1486 Europe driven by temperature change. *Climate of the Past*, *17*(5), 1903-1918.
1487 Lehmann, H. (1936). Morphologische Studien auf Java: Geog. Abhandlungen, III, Stuttgart
1488 1954, 144.
1489 Liu, Z., Groves, C., Yuan, D., Meiman, J., Jiang, G., He, S., et al. (2004). Hydrochemical
1490 variations during flood pulses in the south-west China peak cluster karst: impacts of CaCO3–
1491 H2O–CO2 interactions. *Hydrol. Process., 18*, 2423–2437. https://doi.org/10.1002/hyp.1472
1492 Liu, Z., Li, Q., Sun, H., & Wang, J. (2007). Seasonal, diurnal and storm-scale hydrochemical
1493 variations of typical epikarst springs in subtropical karst areas of SW China: Soil CO2 and
1494 dilution effects. *Journal of Hydrology, 337*, 207–223.
1495 https://doi.org/10.1016/j.jhydrol.2007.01.034
1496 Long, K. E., Schneider, L., Connor, S. E., Shulmeister, N., Finn, J., Roberts, G. L., ... & Haberle,
1497 S. G. (2021). Human impacts and Anthropocene environmental change at Lake Kutubu, a
1498 Ramsar wetland in Papua New Guinea. *Proceedings of the National Academy of Sciences*,
1499 *118*(40), e2022216118.

Lowe, D.J., & Gunn, J. (1997). Carbonate speleogenesis: An inception horizon hypothesis. *Acta Carsologica*, *38*, 457–488.

Lucha, P., Gutiérrez, F., Galve, J. P., & Guerrero, J. (2012). Geomorphic and stratigraphic evidence of incision-induced halokinetic uplift and dissolution subsidence in transverse drainages crossing the evaporite-cored Barbastro–Balaguer Anticline (Ebro Basin, NE Spain). *Geomorphology*, *171*, 154-172. https://doi.org/10.1016/j.geomorph.2012.05.015.

Macpherson, G.L., & Sullivan, P.L. (2019a). Watershed-scale chemical weathering in a merokarst terrain, northeastern Kansas, USA. *Chemical Geology*, *527*, 118988. https://doi.org/10.1016/j.chemgeo.2018.12.001

Macpherson, G.L., & Sullivan, P.L. (2019b). Dust, impure calcite, and phytoliths: Modeled alternative sources of chemical weathering solutes in shallow groundwater. *Chemical Geology*, *527*, 118871. https://doi.org/10.1016/j.chemgeo.2018.08.007

Martin, J.B. (2017). Carbonate minerals in the global carbon cycle. *Chemical Geology*, *449*, 58–72. https://doi.org/10.1016/j.chemgeo.2016.11.029

Martin, J.B., & Dean, R.W. (1999). Temperature as a natural tracer of short residence times for groundwater in karst aquifers. *Karst Modeling. Karst Waters Institute Special Publication*, 5, 236–242.

Martin, J.B., & Dean, R.W. (2001). Exchange of water between conduits and matrix in the Floridan aquifer. *Chemical Geology*, *179*, 145–165. https://doi.org/10.1016/S0009-2541(01)00320-5

Martin, J. B., Gulley, J., & Spellman, P. (2012). Tidal pumping of water between Bahamian blue holes, aquifers, and the ocean. *Journal of Hydrology*, *416*, 28-38.

Martin, J. B., deGrammont, P. C., Covington, M. D., & Toran, L. (2021). A new focus on the

neglected carbonate critical zone. EOS, 102.

Mattey, D.P., Atkinson, T.C., Barker, J.A., Fisher, R., Latin, J.-P., Durrell, R., et al. (2016). Carbon dioxide, ground air and carbon cycling in Gibraltar karst. *Geochimica et Cosmochimica Acta*, *184*, 88–113. https://doi.org/10.1016/j.gca.2016.01.041

Mijares, A. S., Détroit, F., Piper, P., Grün, R., Bellwood, P., Aubert, M., ... & Dizon, E. (2010). New evidence for a 67,000-year-old human presence at Callao Cave, Luzon, Philippines. *Journal of human evolution*, *59*(1), 123-132.

Milanolo, S., & Gabrovšek, F. (2009). Analysis of Carbon Dioxide Variations in the Atmosphere of Srednja Bijambarska Cave, Bosnia and Herzegovina. *Boundary-Layer Meteorol, 131*, 479–493. https://doi.org/10.1007/s10546-009-9375-5

Miorandi, R., Borsato, A., Frisia, S., Fairchild, I.J., & Richter, D.K. (2010). Epikarst hydrology and implications for stalagmite capture of climate changes at Grotta di Ernesto (NE Italy): results from long-term monitoring. *Hydrol. Process., 24,* 3101–3114. https://doi.org/10.1002/hyp.7744

Monroe, W.H. (1976). The karst landforms of Puerto Rico (No. 899). US Geological Survey.

Moore, O.W., Buss, H.L., Green, S.M., Liu, M., & Song, Z. (2017). The importance of non-carbonate mineral weathering as a soil formation mechanism within a karst weathering profile in the SPECTRA Critical Zone Observatory, Guizhou Province, China. *Acta Geochim, 36*, 566–571. https://doi.org/10.1007/s11631-017-0237-4

Moyes, H., Awe, J. J., Brook, G. A., & Webster, J. W. (2009). The ancient Maya drought cult: Late Classic cave use in Belize. *Latin American Antiquity*, *20*(1), 175-206.

Musgrove, M., & Banner, J.L. (2004). Controls on the spatial and temporal variability of vadose dripwater geochemistry: Edwards aquifer, central Texas, *Geochimica et Cosmochimica Acta, 68,* 1007–1020. https://doi.org/10.1016/j.gca.2003.08.014

1546 Mylroie, J.E., & Carew, J.L. (1990). The flank margin model for dissolution cave development
1547 in carbonate platforms. *Earth Surface Processes and Landforms, 15*, 413–424.
1548 National Research Council (2001). *Basic research opportunities in earth science.* National
1549 Academies Press.
1550 Newton, J. G. (1987). *Development of sinkholes resulting from man's activities in the eastern*
1551 *United States* (Vol. 958). US Geological Survey.
1552 Noronha, A. L., Johnson, K. R., Southon, J. R., Hu, C., Ruan, J., & McCabe-Glynn, S. (2015).
1553 Radiocarbon evidence for decomposition of aged organic matter in the vadose zone as the main
1554 source of speleothem carbon. *Quaternary Science Reviews*, *127*, 37-47.
1555 Opdyke, N. D., Spangler, D. P., Smith, D. L., Jones, D. S., & Lindquist, R. C. (1984). Origin of
1556 the epeirogenic uplift of Pliocene-Pleistocene beach ridges in Florida and development of the
1557 Florida karst. *Geology*, *12*(4), 226-228.
1558 Oster, J. L., Covey, A. K., Lawrence, C. R., Giannetta, M. G., & Druhan, J. L. (2021). A reactive
1559 transport approach to modeling cave seepage water chemistry II: Elemental signatures.
1560 *Geochimica et Cosmochimica Acta*, 311, 353-373.
1561 Ott, R. F., Gallen, S. F., Caves Rugenstein, J. K., Ivy-Ochs, S., Helman, D., Fassoulas, C., et al.
1562 (2019). Chemical versus mechanical denudation in meta-clastic and carbonate bedrock
1563 catchments on Crete, Greece, and mechanisms for steep and high carbonate topography. *Journal*
1564 *of Geophysical Research: Earth Surface*, *124*(12), 2943-2961.
1565 Ott, R. F. (2020). How lithology impacts global topography, vegetation, and animal biodiversity:
1566 A global-scale analysis of mountainous regions. *Geophysical Research Letters, 47*(20),
1567 e2020GL088649.

1568 Palmer, A.N. (1991). Origin and morphology of limestone caves. *GSA Bulletin*, *103*, 1–21.
1569 https://doi.org/10.1130/0016-7606(1991)103<0001:OAMOLC>2.3.CO;2
1570 Palmer, A.N. (2001). Dynamics of cave development by allogenic water. *Acta carsologica*, *30*,
1571 13–32.
1572 Pané, F. R. (1999). An Account of the Antiquities of the Indians: A New Edition, with an
1573 Introductory Study, Notes, and Appendices by José Juan Arrom. Duke University Press.
1574 Panno, S. V., Kelly, W. R., Scott, J., Zheng, W., McNeish, R. E., Holm, N., ... & Baranski, E. L.
1575 (2019). Microplastic contamination in karst groundwater systems. *Groundwater*, *57*(2), 189-196.
1576 Parise, M., Ravbar, N., Živanović, V., Mikszewski, A., Kresic, N., Mádl-Szőnyi, J., & Kukurić,
1577 N. (2015). Hazards in karst and managing water resources quality. In *Karst aquifers—*
1578 *Characterization and engineering* (pp. 601-687). Springer, Cham.
1579 Patton, N.R., Lohse, K.A., Godsey, S.E., Crosby, B.T., & Seyfried, M.S. (2018). Predicting soil
1580 thickness on soil mantled hillslopes. *Nature Communications*, *9*, 3329.
1581 https://doi.org/10.1038/s41467-018-05743-y
1582 Perrin, A. S., Probst, A., & Probst, J. L. (2008). Impact of nitrogenous fertilizers on carbonate
1583 dissolution in small agricultural catchments: Implications for weathering CO2 uptake at regional
1584 and global scales. *Geochimica et Cosmochimica Acta*, *72*(13), 3105-3123.
1585 Peterson, E.W., Wicks, C.M., 2005. Fluid and solute transport from a conduit to the matrix in a
1586 carbonate aquifer system. Mathematical Geology, 37, 851-867,
1587 Phillips, J.D., Pawlik, Ł., & Šamonil, P. (2019). Weathering fronts. *Earth-Science Reviews*, *198*,
1588 102925. https://doi.org/10.1016/j.earscirev.2019.102925

1589 Pickering, R., Kramers, J. D., Hancox, P. J., de Ruiter, D. J., & Woodhead, J. D. (2011).
1590 Contemporary flowstone development links early hominin bearing cave deposits in South Africa.
1591 *Earth and planetary science letters*, *306*(1-2), 23-32.
1592 Plummer, L.N. (1975). Mixing of sea water with calcium carbonate ground water. *Geological*
1593 *Society of America Memoir*, *142*, 219–236.
1594 Plummer, L. N., Wigley, T. M. L., & Parkhurst, D. L. (1978). The kinetics of calcite dissolution
1595 in CO 2-water systems at 5 degrees to 60 degrees C and 0.0 to 1.0 atm CO2. *American journal of*
1596 *science*, *278*(2), 179-216. https://doi.org/10.2475/ajs.278.2.179
1597 Plummer, L.N., Parkhurst, D.L., & Wigley, T.M.L. (1979). Critical review of the kinetics of
1598 calcite dissolution and precipitation. In *Chemical Modeling in Aqueous Systems.* ACS
1599 Publications, 537-573.
1600 Querejeta, J. I., Estrada-Medina, H., Allen, M. F., & Jiménez-Osornio, J. J. (2007). Water source
1601 partitioning among trees growing on shallow karst soils in a seasonally dry tropical climate.
1602 *Oecologia*, *152*, 26–36.
1603 Quine, T., Guo, D., Green, S. M., Tu, C., Hartley, I., Zhang, X., ... & Meersmans, J. (2017).
1604 Ecosystem service delivery in Karst landscapes: anthropogenic perturbation and recovery. *Acta*
1605 *Geochimica*, 36(3), 416-420.
1606 Quinlan, J. F., Davies, G. J., Jones, S. W., & Huntoon, P. W. (1996). The applicability of
1607 numerical models to adequately characterize ground-water flow in karstic and other triple-
1608 porosity aquifers. *Subsurface fluid-flow (ground-water and vadose zone) modeling, ASTM STP*,
1609 *1288*, 114-133.
1610 Reich, P. B., & Borchert, R. (1984). Water stress and tree phenology in a tropical dry forest in
1611 the lowlands of Costa Rica. *Journal of Ecology*, *72*, 61-74.

1612 Rempe, D.M., & Dietrich, W.E. (2014). A bottom-up control on fresh-bedrock topography under
1613 landscapes. *Proceedings of the National Academy of Sciences, 111*, 6576–6581.
1614 https://doi.org/10.1073/pnas.1404763111
1615 Riebe, C.S., Hahm, W.J., & Brantley, S.L. (2017). Controls on deep critical zone architecture: a
1616 historical review and four testable hypotheses. *Earth Surface Processes and Landforms, 42*, 128–
1617 156. https://doi.org/10.1002/esp.4052
1618 Roland, M., Serrano-Ortiz, P., Kowalski, A. S., Goddéris, Y., Sánchez-Cañete, E. P., Ciais, P., ...
1619 & Janssens, I. A. (2013). Atmospheric turbulence triggers pronounced diel pattern in karst
1620 carbonate geochemistry. Biogeosciences, 10(7), 5009-5017.
1621 Romero-Mujalli, G., Hartmann, J., Börker, J., Gaillardet, J., & Calmels, D. (2019). Ecosystem
1622 controlled soil-rock pCO2 and carbonate weathering – Constraints by temperature and soil water
1623 content. *Chemical Geology, 527*, 118634. https://doi.org/10.1016/j.chemgeo.2018.01.030
1624 Rossinsky, V., & Wanless, H. R. (1992). Topographic and vegetative controls on calcrete
1625 formation, Turks and Caicos Islands, British West Indies. *Journal of Sedimentary Research,*
1626 *62*(1), 84-98.
1627 Ryb, U., Matmon, A., Erel, Y., Haviv, I., Katz, A., Starinsky, A., et al. (2014). Controls on
1628 denudation rates in tectonically stable Mediterranean carbonate terrain. *Geological Society of*
1629 *America Bulletin, 126*, 553–568. https://doi.org/10.1130/B30886.1
1630 Sanchez-Cañete, E. P., Serrano-Ortiz, P., Kowalski, A. S., Oyonarte, C., & Domingo, F. (2011).
1631 Subterranean CO2 ventilation and its role in the net ecosystem carbon balance of a karstic
1632 shrubland. *Geophysical research letters*, *38*(9). https://doi.org/10.1029/2011GL047077
1633 Schulze-Makuch, D., Carlson, D. A., Cherkauer, D. S., & Malik, P. (1999). Scale dependency of
1634 hydraulic conductivity in heterogeneous media. *Ground Water*, *37*(8), 904-919.

1635 Scribner, C. A., Martin, E. E., Martin, J. B., Deuerling, K. M., Collazo, D. F., & Marshall, A. T.
1636 (2015). Exposure age and climate controls on weathering in deglaciated watersheds of western
1637 Greenland. *Geochimica et Cosmochimica Acta*, *170*, 157-172.
1638 Sekhon, N., Novello, V. F., Cruz, F. W., Wortham, B. E., Ribeiro, T. G., & Breecker, D. O.
1639 (2021). Diurnal to seasonal ventilation in Brazilian caves. Global and Planetary Change, 197,
1640 103378.
1641 Shaughnessy, A. R., Gu, X., Wen, T., & Brantley, S. L. (2021). Machine learning deciphers
1642 CO2 sequestration and subsurface flowpaths from stream chemistry. *Hydrology and*
1643 *Earth System Sciences*, *25*(6), 3397-3409.
1644 Siemers, J., & Dreybrodt, W. (1998). Early development of Karst aquifers on percolation
1645 networks of fractures in limestone. *Water Resour. Res.*, *34*, 409–419.
1646 https://doi.org/10.1029/97WR03218
1647 Simms, M.J. (2004). Tortoises and hares: dissolution, erosion and isostasy in landscape
1648 evolution. *Earth Surf. Process. Landforms, 29,* 477–494. https://doi.org/10.1002/esp.1047
1649 Smith, D.I., & Atkinson, T.C. (1976). Process, Landforms and Climate in Limestone Regions.
1650 *Geomorphology and climate, 512*.
1651 Smart, P., Waltham, T., Yang, M., & Zhang, Y. J. (1986). Karst geomorphology of western
1652 Guizhou, China. *Cave Science*, *13*(3).
1653 Spalding, R. F., & Mathews, T. D. (1972). Stalagmites from caves in the Bahamas: Indicators of
1654 low sea level stand. *Quaternary Research*, 2(4), 470-472.
1655 Spellman, P., Gulley, J., Martin, J. B., & Loucks, J. (2019). The role of antecedent groundwater
1656 heads in controlling transient aquifer storage and flood peak attenuation in karst watersheds.
1657 *Earth Surface Processes and Landforms*, *44*(1), 77-87.

1658 Spötl, C., Fairchild, I. J., & Tooth, A. F. (2005). Cave air control on dripwater geochemistry,
1659 Obir Caves (Austria): Implications for speleothem deposition in dynamically ventilated caves.
1660 *Geochimica et Cosmochimica Acta*, *69*(10), 2451-2468.
1661 https://doi.org/10.1016/j.gca.2004.12.009
1662 Stevanović, Z. (2018). Global distribution and use of water from karst aquifers. *Geological*
1663 *Society, London, Special Publications*, *466*(1), 217-236.
1664 Stock, G.M., Granger, D.E., Sasowsky, I.D., Anderson, R.S., & Finkel, R.C. (2005). Comparison
1665 of U–Th, paleomagnetism, and cosmogenic burial methods for dating caves: implications for
1666 landscape evolution studies. *Earth and Planetary Science Letters*, *236*(1-2), 388-403.
1667 Stoll, H. M., Müller, W., & Prieto, M. (2012). I-STAL, a model for interpretation of Mg/Ca,
1668 Sr/Ca and Ba/Ca variations in speleothems and its forward and inverse application on seasonal to
1669 millennial scales. *Geochemistry, Geophysics, Geosystems*, *13*(9).
1670 Stoll, H. M., Cacho, I., Gasson, E., Sliwinski, J., Kost, O., Moreno, A., ... & Edwards, R. L.
1671 (2022). Rapid northern hemisphere ice sheet melting during the penultimate deglaciation. *Nature*
1672 *communications*, *13*(1), 1-16.
1673 Ström, L., Owen, A. G., Godbold, D. L., & Jones, D. L. (2005). Organic acid behaviour in a
1674 calcareous soil implications for rhizosphere nutrient cycling. *Soil Biology & Biochemistry*, *37*,
1675 2046–2054.
1676 Sullivan, P.L., Stops, M.W., Macpherson, G.L., Li, L., Hirmas, D.R., & Dodds, W.K. (2019).
1677 How landscape heterogeneity governs stream water concentration-discharge behavior in
1678 carbonate terrains (Konza Prairie, USA). *Chemical Geology*, *527*, 118989.
1679 https://doi.org/10.1016/j.chemgeo.2018.12.002

1680 Sullivan, P.L., Wymore, A.S., McDowell, M., Aarons, S., Aciego, S., Anders, A.M., et al.
1681 (2017). New opportunities for Critical Zone science, In: *2017 CZO Arlington Meeting White*
1682 *Booklet*.
1683 Sullivan, P. L., Zhang, C., Behm, M., Zhang, F., & Macpherson, G. L. (2020). Toward a new
1684 conceptual model for groundwater flow in merokarst systems: Insights from multiple
1685 geophysical approaches. *Hydrological Processes*, *34*(24), 4697-4711.
1686 Surić, M., Richards, D. A., Hoffmann, D. L., Tibljaš, D., & Juračić, M. (2009). Sea-level change
1687 during MIS 5a based on submerged speleothems from the eastern Adriatic Sea (Croatia). *Marine*
1688 *Geology*, 262(1-4), 62-67.
1689 Sutikna, T., Tocheri, M. W., Morwood, M. J., Saptomo, E. W., Awe, R. D., Wasisto, S., ... &
1690 Roberts, R. G. (2016). Revised stratigraphy and chronology for Homo floresiensis at Liang Bua
1691 in Indonesia. *Nature*, *532*(7599), 366-369.
1692 Svensson, U., & Dreybrodt, W. (1992). Dissolution kinetics of natural calcite minerals in CO2-
1693 water systems approaching calcite equilibrium. *Chemical Geology, 100*, 129–145.
1694 Swaffer, B. A., Holland, K. L., Doody, T. M., Li, C., & Hutson, J. (2014). Water use strategies of
1695 two co-occurring tree species in a semi-arid karst environment. *Hydrological Processes*, *28*,
1696 2003–2017.
1697 Szymczak, P., & Ladd, A.J.C. (2011). The initial stages of cave formation: Beyond the one-
1698 dimensional paradigm. *Earth and Planetary Science Letters, 301*, 424–432.
1699 Szymczak, P., & Ladd, A.J.C. (2012). Reactive-infiltration instabilities in rocks. Fracture
1700 dissolution. *J. Fluid Mech., 702*, 239–264. https://doi.org/10.1017/jfm.2012.174
1701 https://doi.org/10.1016/j.epsl.2010.10.026

1702 Tennyson, R., Brahana, V., Polyak, V.J., Potra, A., Covington, M., Asmerom, Y., et al. (2017).
1703 Hypogene Speleogenesis in the Southern Ozark Uplands, Mid-Continental United States, In:
1704 Klimchouk, A. N., Palmer, A., De Waele, J., S. Auler, A., & Audra, P. (Eds.), Hypogene Karst
1705 Regions and Caves of the World. Springer International Publishing, Cham, pp. 663–676.
1706 https://doi.org/10.1007/978-3-319-53348-3_43
1707 Tobin, B. W., Polk, J. S., Arpin, S. M., Shelley, A., & Taylor, C. (2021). A conceptual model of
1708 epikarst processes across sites, seasons, and storm events. *Journal of Hydrology*, 596, 125692.
1709 Tooth, A.F., & Fairchild, I.J. (2003). Soil and karst aquifer hydrological controls on the
1710 geochemical evolution of speleothem-forming drip waters, Crag Cave, southwest Ireland.
1711 *Journal of Hydrology, 273*, 51–68. https://doi.org/10.1016/S0022-1694(02)00349-9
1712 Torres, M. A., A. J. West, & Li, G. (2014). Sulphide oxidation and carbonate dissolution as a
1713 source of CO2 over geological timescales, *Nature, 507*(7492), 346-349.
1714 Treble, P. C., Baker, A., Abram, N. J., Hellstrom, J. C., Crawford, J., Gagan, M. K., ... &
1715 Paterson, D. (2022). Ubiquitous karst hydrological control on speleothem oxygen isotope
1716 variability in a global study. *Communications Earth & Environment*, *3*(1), 1-10.
1717 Troester, J. W., White, E. L., & White, W. B. (1984). A comparison of sinkhole depth frequency
1718 distributions in temperate and tropic karst regions. In *Multidisciplinary conference on sinkholes.*
1719 *1* (pp. 65-73).
1720 Vacher, H.L., & Mylroie, J.E. (2002). Eogenetic karst from the perspective of an equivalent
1721 porous medium. *Carbonates and Evaporites*, *17*, 182.
1722 Veni, G., DuChene, H., & Groves, C. (2001). Living with Karst: A Fragile
1723 Foundation—American Geological Institute Environmental Awareness Series 4. *American*
1724 *Geological Institute, Alexandria*, 7.

1725 Vesper, D. J., & White, W. B. (2003). Metal transport to karst springs during storm flow: an
1726 example from Fort Campbell, Kentucky/Tennessee, USA. *Journal of Hydrology*, *276*(1-4), 20-
1727 36.
1728 Vesper, D. J., & White, W. B. (2004). Storm pulse chemographs of saturation index and carbon
1729 dioxide pressure: implications for shifting recharge sources during storm events in the karst
1730 aquifer at Fort Campbell, Kentucky/Tennessee, USA. *Hydrogeology Journal*, *12*(2), 135-143.
1731 https://doi.org/10.1007/s10040-003-0299-8
1732 Wagner, T., Fritz, H., Stüwe, K., Nestroy, O., Rodnight, H., Hellstrom, J., et al. 2(011).
1733 Correlations of cave levels, stream terraces and planation surfaces along the River Mur—Timing
1734 of landscape evolution along the eastern margin of the Alps. *Geomorphology*, *134*, 62–78.
1735 https://doi.org/10.1016/j.geomorph.2011.04.024
1736 Waltham, T. (2008). Sinkhole hazard case histories in karst terrains. *Quarterly Journal of*
1737 *Engineering Geology and Hydrogeology*, *41*(3), 291-300.
1738 Wen, H., Sullivan, P. L., Macpherson, G. L., Billings, S. A., & Li, L. (2021). Deepening roots
1739 can enhance carbonate weathering by amplifying CO 2-rich recharge. *Biogeosciences*, *18*(1), 55-
1740 75.
1741 White, W.B. (2002). Karst hydrology: recent developments and open questions. *Engineering*
1742 *Geology, 65*, 85–105. https://doi.org/10.1016/S0013-7952(01)00116-8
1743 White, W.B. (1984). Rate processes: chemical kinetics and karst landform development. In
1744 *Groundwater as a Geomorphic Agent*. Routledge: London.
1745 https://doi.org/10.4324/9781003028833
1746 White, W.B., Herman, E., Rutigliano, M., Herman, J., Vesper, D., & Engel, S. (2016). Karst
1747 groundwater contamination and public health. *Karst Waters Inst. Spec. Publ. 19*, Springer.

White, W.B., & White, E.L. (2005). Size scales for closed depression landforms: The place of tiankengs. *Cave and Karst Science, 32*(2/3), 111.

Wigley, T.M.L., & Plummer, L.N. (1976). Mixing of carbonate waters. *Geochimica et Cosmochimica Acta, 40*, 989–995. https://doi.org/10.1016/0016-7037(76)90041-7

Williams, P. (2008a). The role of the epikarst in karst and cave hydrogeology: a review. *International Journal of Speleology, 37*. http://dx.doi.org/10.5038/1827-806X.37.1.1

Williams, P. (2008b). *World Heritage Caves and Karst: A thematic study*. Gland, Switzerland: IUCN 57pp.

Williams, P.W. (1985). Subcutaneous hydrology and the development of doline and cockpit karst. *Zeitschrift für Geomorphologie, 29*, 463–482.

Wilson, D. J., Von Strandmann, P. A. P., White, J., Tarbuck, G., Marca, A. D., Atkinson, T. C., & Hopley, P. J. (2021). Seasonal variability in silicate weathering signatures recorded by Li isotopes in cave drip-waters. *Geochimica et Cosmochimica Acta*, 312, 194-216.

Wolfe, B. T., & Kursar, T. A. (2015). Diverse patterns of stored water use among saplings in seasonally dry tropical forests. *Oecologia, 179*, 925–936.

Wong, C.I., Banner, J.L., & Musgrove, M. (2011). Seasonal dripwater Mg/Ca and Sr/Ca variations driven by cave ventilation: Implications for and modeling of speleothem paleoclimate records. *Geochimica et Cosmochimica Acta, 75*, 3514–3529. https://doi.org/10.1016/j.gca.2011.03.025

Wood, W.W. (1985). Origin of caves and other solution openings in the unsaturated (vadose) zone of carbonate rocks: A model for CO2 generation. *Geology, 13*, 822–824.

Wood, W.W., & Petraitis, M.J. (1984). Origin and Distribution of Carbon Dioxide in the Unsaturated Zone of the Southern High Plains of Texas. *Water Resour. Res., 20*, 1193–1208. https://doi.org/10.1029/WR020i009p01193

Worthington, S.R. (1999). A comprehensive strategy for understanding flow in carbonate aquifers, in: *Karst Modeling, Karst Waters Institute Special Publication 5. Karst Waters Institute*, pp. 30–37.

Worthington, S.R.H. (2009). Diagnostic hydrogeologic characteristics of a karst aquifer (Kentucky, USA). *Hydrogeol J, 17*, 1665–1678. https://doi.org/10.1007/s10040-009-0489-0

Worthington, S.R.H., Davies, G.J., & Alexander, E.C. (2016). Enhancement of bedrock permeability by weathering. *Earth-Science Reviews, 160*, 188–202. https://doi.org/10.1016/j.earscirev.2016.07.002

Wray, R.A.L., & Sauro, F. (2017). An updated global review of solutional weathering processes and forms in quartz sandstones and quartzites. *Earth-Science Reviews, 171*, 520–557. https://doi.org/10.1016/j.earscirev.2017.06.008

Yizhaq, H., Ish-Shalom, C., Raz, E., & Ashkenazy, Y. (2017). Scale-free distribution of Dead Sea sinkholes: Observations and modeling. *Geophysical Research Letters*, *44*(10), 4944-4952.

Zanolli, C., Davies, T. W., Joannes-Boyau, R., Beaudet, A., Bruxelles, L., de Beer, F., ... & Skinner, M. M. (2022). Dental data challenge the ubiquitous presence of Homo in the Cradle of Humankind. *Proceedings of the National Academy of Sciences*, *119*(28), e2111212119.

Zeng, Q., Liu, Z., Chen, B., Hu, Y., Zeng, S., Zeng, C., et al. (2017). Carbonate weathering-related carbon sink fluxes under different land uses: A case study from the Shawan Simulation Test Site, Puding, Southwest China. *Chemical Geology, 474*, 58–71.

1791 Zhao, L., & Hou, R. (2019). Human causes of soil loss in rural karst environments: a case study
1792 of Guizhou, China. *Scientific Reports*, *9*(1), 1-11. doi:10.1038/s41598-018-35808-3
1793 Zhao, S., Pereira, P., Wu, X., Zhou, J., Cao, J., & Zhang, W. (2020). Global karst vegetation
1794 regime and its response to climate change and human activities. *Ecological Indicators*, *113*,
1795 106208.
1796 Zorn, M., Erhartic, B., Komac, B., & Gauchon, C. (2009). La Slovénie, berceau du géotourisme
1797 karstique. *Karstologia*, *54*(1), 1–10. https://doi.org/10.3406/karst.2009.2655